

# On the Enthalpy of Formation of Hydroxyl Radical and Gas-Phase Bond Dissociation Energies of Water and Hydroxyl

Branko Ruscic,<sup>\*,†</sup> Albert F. Wagner,<sup>†</sup> Lawrence B. Harding,<sup>†</sup> Robert L. Asher,<sup>†</sup> David Feller,<sup>‡</sup> David A. Dixon,<sup>\*,‡</sup> Kirk A. Peterson,<sup>‡,§</sup> Yang Song,<sup>||</sup> Ximei Qian,<sup>||</sup> Cheuk-Yiu Ng,<sup>\*,||</sup> Jianbo Liu,<sup>⊥</sup> Wenwu Chen,<sup>⊥</sup> and David W. Schwenke<sup>#</sup>

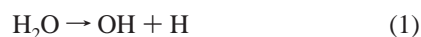
Chemistry Division, Argonne National Laboratory, Argonne, Illinois 60439-4831, William R. Wiley Environmental Molecular Sciences Laboratory, Pacific Northwest National Laboratory, Richland, Washington 99352, Department of Chemistry, Washington State University, Richland, Washington 99352, Ames Laboratory, USDOE, and Department of Chemistry, Iowa State University, Ames, Iowa 50011, Lawrence Berkeley National Laboratory, Chemical Science Division, Berkeley, California 94720, and NASA Ames Research Center, Moffett Field, California 94035-1000

Received: October 22, 2001

In a recent letter (*J. Phys. Chem. A*, **2001**, *105*,1), we argued that, although all major thermochemical tables recommend a value of  $\Delta H_{10}^{\circ}(\text{OH})$  based on a spectroscopic approach, the correct value is 0.5 kcal/mol lower as determined from an ion cycle. In this paper, we expand upon and augment both the experimental and theoretical arguments presented in the letter. In particular, three separate experiments (mass-selected photoionization measurements, pulsed-field-ionization photoelectron spectroscopy measurements, and photoelectron-photoion coincidence measurements) utilizing the positive ion cycle to derive the O–H bond energy are shown to converge to a consensus value of the appearance energy  $\text{AE}_0(\text{OH}^+/\text{H}_2\text{O}) = 146117 \pm 24 \text{ cm}^{-1}$  ( $18.116_2 \pm 0.003_0 \text{ eV}$ ). With the most accurate currently available zero kinetic energy photoionization value for the ionization energy  $\text{IE}(\text{OH}) = 104989 \pm 2 \text{ cm}^{-1}$ , corroborated by a number of photoelectron measurements, this leads to  $D_0(\text{H–OH}) = 41128 \pm 24 \text{ cm}^{-1} = 117.59 \pm 0.07 \text{ kcal/mol}$ . This corresponds to  $\Delta H_{10}^{\circ}(\text{OH}) = 8.85 \pm 0.07 \text{ kcal/mol}$  and implies  $D_0(\text{OH}) = 35593 \pm 24 \text{ cm}^{-1} = 101.76 \pm 0.07 \text{ kcal/mol}$ . These results are completely supported by the most sophisticated theoretical calculations ever performed on the  $\text{H}_2\text{O}$  system, CCSD(T)/aug-cc-pVnZ,  $n = \text{Q}, 5, 6, \text{ and } 7$ , extrapolated to the CBS limit and including corrections for core-valence effects, scalar relativistic effects, incomplete correlation recovery, and diagonal Born–Oppenheimer corrections. These calculations have an estimated theoretical error of  $\leq 0.2 \text{ kcal/mol}$  based on basis set convergence properties. They reproduce the experimental results for dissociation energies, atomization energies, and ionization energies for the  $\text{H}_2\text{O}$  system to within 0.0–0.2 kcal/mol. In contrast, the previously accepted values of the two successive bond dissociation energies of water differ from the current values by 0.5 kcal/mol. These values were derived from the spectroscopic determinations of  $D_0(\text{OH})$  using a very short Birge–Sponer extrapolation on  $\text{OH}/\text{OD } A^1\Sigma^+$ . However, on the basis of a calculation of the A state potential energy curve (with a multireference single and double excitation wave function and an aug-cc-pV5Z basis set) and an exhaustive reanalysis of the original measured data on both the A and B states of OH, the Birge–Sponer extrapolation can be demonstrated to significantly underestimate the bond dissociation energy, although only the last vibrational level was not observed experimentally. The recommended values of this paper affect a large number of other thermochemical quantities which directly or indirectly rely on or refer to  $D_0(\text{H–OH})$ ,  $D_0(\text{OH})$ , or  $\Delta H_{10}^{\circ}(\text{OH})$ . This is illustrated by an analysis of several reaction enthalpies, deprotonation enthalpies, and proton affinities.

## 1. Introduction

It is difficult to name many thermochemical quantities that are more fundamental to chemistry than the O–H bond dissociation energy in water,  $D_0(\text{H–OH}) \equiv \Delta H_{10}^{\circ}(\text{OH})$  (1):



Its prominence arises from its ubiquity, which covers the full

spectrum from simple (though fundamental) chemical reactions, in which this bond is formed and/or destroyed, to the extremes of complex environments, such as flames or the troposphere, where the balance between production and consumption of hydroxyl radicals is an important factor shaping the overall chemistry. This bond energy, or, equivalently, the enthalpy of formation of hydroxyl radical,  $\Delta H_{10}^{\circ}(\text{OH})$  (vide infra), is one of the fundamental building blocks in models that describe such systems. In particular, models describing flames or the atmosphere typically include a very large number of intertwined chemical reactions, and their predictive ability can be quite sensitive to minute inaccuracies in the enthalpies of formation of key intermediate species, such as OH. Moreover, the significance of OH transcends the chemical reactions in which

\* To whom correspondence should be addressed. e-mail: ruscic@anl.gov

† Argonne National Laboratory.

‡ Pacific Northwest National Laboratory.

§ Washington State University.

|| Iowa State University.

⊥ Lawrence Berkeley National Laboratory.

# NASA Ames Research Center.

**TABLE 1: Various Values for the 0 K Enthalpy of Formation of OH and Related Values for  $D_0(\text{H-OH})$  and  $D_0(\text{OH})^a$** 

source	$\Delta H_{\text{f}}^{\circ}(\text{OH})$	$D_0(\text{H-OH})$	$D_0(\text{OH})$
Gurvich et al., <sup>b</sup> following Carlone and Dalby <sup>c</sup> Barrow <sup>f</sup>	$9.35 \pm 0.05$ kcal/mol <sup>d</sup>	$118.08 \pm 0.05$ kcal/mol <sup>e</sup> (41301 $\pm$ 17 cm <sup>-1</sup> )	$101.27 \pm 0.04$ kcal/mol (35420 $\pm$ 15 cm <sup>-1</sup> )
JANAF <sup>g</sup>	$9.26 \pm 0.29$ kcal/mol <sup>d</sup>	$118.00 \pm 0.29$ kcal/mol <sup>e</sup> (41270 $\pm$ 100 cm <sup>-1</sup> )	$101.36 \pm 0.29$ kcal/mol (35450 $\pm$ 100 cm <sup>-1</sup> )
positive ion cycle, literature value <sup>l</sup>	$9.18 \pm 0.29$ kcal/mol	$117.91 \pm 0.29$ kcal/mol <sup>e</sup> (41240 $\pm$ 100 cm <sup>-1</sup> )	$101.44 \pm 0.29$ kcal/mol <sup>h</sup> (35480 $\pm$ 100 cm <sup>-1</sup> )
positive ion cycle, PIMS experiment <sup>l</sup>	$8.83 \pm 0.18$ kcal/mol <sup>i</sup>	$117.56 \pm 0.18$ kcal/mol (41118 $\pm$ 65 cm <sup>-1</sup> )	$101.79 \pm 0.19$ kcal/mol <sup>k</sup> (35602 $\pm$ 65 cm <sup>-1</sup> )
positive ion cycle, PFI-PE experiment <sup>m</sup>	$8.85 \pm 0.08$ kcal/mol <sup>i</sup>	$117.59 \pm 0.08$ kcal/mol (41127 $\pm$ 28 cm <sup>-1</sup> )	$101.77 \pm 0.08$ kcal/mol <sup>k</sup> (35594 $\pm$ 29 cm <sup>-1</sup> )
positive ion cycle, PFI-PEPICO experiment <sup>n</sup>	$8.86 \pm 0.05$ kcal/mol <sup>i</sup>	$117.60 \pm 0.05$ kcal/mol (41130 $\pm$ 16 cm <sup>-1</sup> )	$101.76 \pm 0.05$ kcal/mol <sup>k</sup> (35590 $\pm$ 18 cm <sup>-1</sup> )
photodissociation of H <sub>2</sub> O using H atom Rydberg "tagging" TOF technique <sup>o</sup>	$8.83 \pm 0.12$ kcal/mol <sup>i</sup>	$117.56 \pm 0.12$ kcal/mol (41118 $\pm$ 40 cm <sup>-1</sup> )	$101.79 \pm 0.12$ kcal/mol <sup>k</sup> (35602 $\pm$ 41 cm <sup>-1</sup> )
present ab initio calculations	$8.92 \pm 0.03$ kcal/mol <sup>i</sup>	$117.66 \pm 0.01$ kcal/mol (41151 $\pm$ 5 cm <sup>-1</sup> )	$101.70 \pm 0.03$ kcal/mol <sup>k</sup> (35570 $\pm$ 9 cm <sup>-1</sup> )
recommended values from present study	$8.85 \pm 0.18$ kcal/mol	$117.76 \pm 0.15$ kcal/mol <sup>e</sup> (41194 $\pm$ 51 cm <sup>-1</sup> )	$101.77 \pm 0.12$ kcal/mol (35591 $\pm$ 42 cm <sup>-1</sup> )
	$8.85 \pm 0.07$ kcal/mol	$117.59 \pm 0.07$ kcal/mol (41128 $\pm$ 24 cm <sup>-1</sup> )	$101.76 \pm 0.07$ kcal/mol <sup>k</sup> (35593 $\pm$ 25 cm <sup>-1</sup> )

<sup>a</sup> The total atomization energy of water at 0 K is taken to be  $\Delta H_{\text{atomization0}}(\text{H}_2\text{O}) = 219.355 \pm 0.024$  kcal/mol (76721  $\pm$  8 cm<sup>-1</sup>), using  $\Delta H_{\text{f}}^{\circ}(\text{H}_2\text{O}) = -57.104 \pm 0.010$  kcal/mol,  $\Delta H_{\text{f}}^{\circ}(\text{H}) = 51.6337 \pm 0.0014$  kcal/mol, and  $\Delta H_{\text{f}}^{\circ}(\text{O}) = 58.984 \pm 0.021$  kcal/mol from refs 1-7; see also ref 8. <sup>b</sup> Reference 1, corresponds to recommended values in ref 14. <sup>c</sup> Reference 15, spectroscopic determination of  $D_0(\text{OH})$ . <sup>d</sup> From  $D_0(\text{OH})$ ,  $\Delta H_{\text{f}}^{\circ}(\text{H})$ , and  $\Delta H_{\text{f}}^{\circ}(\text{O})$ . <sup>e</sup> From  $\Delta H_{\text{atomization0}}(\text{H}_2\text{O}) - D_0(\text{OH})$ . <sup>f</sup> Reference 16, spectroscopic determination of  $D_0(\text{OH})$ . <sup>g</sup> References 3 and 19, see also ref 17. <sup>h</sup> From  $\Delta H_{\text{f}}^{\circ}(\text{OH})$ ,  $\Delta H_{\text{f}}^{\circ}(\text{H})$ , and  $\Delta H_{\text{f}}^{\circ}(\text{O})$ . <sup>i</sup> Based on  $\text{AE}_0(\text{OH}^+/\text{H}_2\text{O}) = 18.115 \pm 0.001$  eV from ref 23 and  $\text{IE}(\text{OH}) = 104989 \pm 2$  cm<sup>-1</sup> from ref 30. <sup>j</sup> From  $D_0(\text{H-OH})$ ,  $\Delta H_{\text{f}}^{\circ}(\text{H}_2\text{O})$ , and  $\Delta H_{\text{f}}^{\circ}(\text{H})$ . <sup>k</sup> From  $\Delta H_{\text{atomization0}}(\text{H}_2\text{O}) - D_0(\text{H-OH})$ . <sup>l</sup> Based on present PIMS result  $\text{AE}_0(\text{OH}^+/\text{H}_2\text{O}) = 18.116_1 \pm 0.003_5$  eV and  $\text{IE}(\text{OH})$  from ref 30. <sup>m</sup> Based on present PFI-PE result  $\text{AE}_0(\text{OH}^+/\text{H}_2\text{O}) = 18.116_5 \pm 0.002_0$  eV and  $\text{IE}(\text{OH})$  from ref 30. <sup>n</sup> Based on present PFI-PEPICO result  $\text{AE}_0(\text{OH}^+/\text{H}_2\text{O}) = 18.115 \pm 0.005$  eV and  $\text{IE}(\text{OH})$  from ref 30. <sup>o</sup> Based on  $D_0(\text{H-OH}) = 41151 \pm 5$  cm<sup>-1</sup> reported in ref 63.

it directly participates as a reactant or product. Namely, the sequential process of building serious thermochemical tables usually follows the "standard" order of elements: O → H → rare gases → halogens → chalcogens → pnictogens → carbon group → etc., in which  $\Delta H_{\text{f}}^{\circ}(\text{OH})$  enters very early. Hence, the tabulated enthalpies of formation of many other "less fundamental" species depend directly or indirectly on the selected value for  $\Delta H_{\text{f}}^{\circ}(\text{OH})$ .

Two additional thermochemical quantities are tightly related to the bond dissociation energy in water: the bond dissociation energy of the hydroxyl radical (i.e., the second bond dissociation energy in water),  $D_0(\text{OH}) \equiv \Delta H_{\text{f}}^{\circ}(\text{O})$ , and the enthalpy of atomization of water (equivalent to the sum of the two successive gas-phase O-H bond dissociation energies in water),  $\Delta H_{\text{atomiz0}}^{\circ}(\text{H}_2\text{O}) \equiv \Delta H_{\text{f}}^{\circ}(\text{O}) = \Delta H_{\text{f}}^{\circ}(\text{H}) + \Delta H_{\text{f}}^{\circ}(\text{OH}) \equiv D_0(\text{H-OH}) + D_0(\text{OH})$ :



Though not directly experimentally measured, an accurate value for the enthalpy of atomization of water can be deduced from generally accepted<sup>1-9</sup> thermochemical values for  $\Delta H_{\text{f}}^{\circ}(\text{H}_2\text{O})$ ,  $\Delta H_{\text{f}}^{\circ}(\text{O})$ , and  $\Delta H_{\text{f}}^{\circ}(\text{H})$  as  $\Delta H_{\text{atomiz0}}^{\circ}(\text{H}_2\text{O}) = 219.355 \pm 0.024$  kcal/mol, equivalent<sup>10</sup> to 76720.7  $\pm$  8.3 cm<sup>-1</sup>. Given a fixed value for the atomization enthalpy, the three quantities  $D_0(\text{H-OH})$ ,  $D_0(\text{OH})$ , and  $\Delta H_{\text{f}}^{\circ}(\text{OH})$ , have only one degree of freedom. An independent determination of  $D_0(\text{H-OH})$  implies a certain value for  $D_0(\text{OH})$  and vice versa. Either of the two bond dissociation energies can be used to deduce<sup>11</sup>  $\Delta H_{\text{f}}^{\circ}(\text{OH})$ , because a given value for  $\Delta H_{\text{f}}^{\circ}(\text{OH})$  simply implies a particular partition<sup>12</sup> of  $\Delta H_{\text{atomiz0}}^{\circ}(\text{H}_2\text{O})$  into  $D_0(\text{H-OH})$  and  $D_0(\text{OH})$ . If a situation arises where both  $D_0(\text{H-OH})$  and  $D_0(\text{OH})$  are known independently, but their sum does not correspond to  $\Delta H_{\text{atomiz0}}^{\circ}(\text{H}_2\text{O})$  within the propagated error bars, or, com-

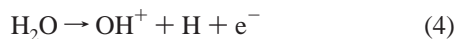
pletely equivalently, if the two bond energies produce conflicting values for  $\Delta H_{\text{f}}^{\circ}(\text{OH})$ , then there must be a problem with at least one of the underlying measurements.

Until we recently produced evidence to the contrary,<sup>13</sup> the best available experimental bond dissociation energy of water was firmly believed<sup>14</sup> to be  $D_0(\text{H-OH}) = 118.08 \pm 0.05$  kcal/mol (see Table 1). The recommended value does not correspond to a direct measurement. Rather, it implicitly originates from the difference  $\Delta H_{\text{atomiz0}}^{\circ}(\text{H}_2\text{O}) - D_0(\text{OH})$ , because it was obtained from  $\Delta H_{\text{f}}^{\circ}(\text{OH}) = 9.347 \pm 0.048$  kcal/mol from Gurvich et al.,<sup>1</sup> which is based on a spectroscopic determination of  $D_0(\text{OH}) = 35420 \pm 15$  cm<sup>-1</sup> by Carlone and Dalby.<sup>15</sup> Without a detailed analysis, the latter value appears to stand on firm ground, because it was obtained by a short (272 cm<sup>-1</sup> beyond the last observed vibrational level) extrapolation of  $\Delta G(v + 1/2)$  of the  $\text{A}^2\Sigma^+$  state of OH, yielding  $D_0(\text{OH}, \text{A}^2\Sigma^+) = 18847 \pm 15$  cm<sup>-1</sup> to  $\text{O } ^1\text{D}_2$ . An even shorter extrapolation (114 cm<sup>-1</sup> beyond the last observed level) led to an apparently congruent value for the dissociation energy of OD.

As opposed to the tabulation of Gurvich et al.,<sup>1</sup> the JANAF Tables<sup>3</sup> list a lower value,  $\Delta H_{\text{f}}^{\circ}(\text{OH}) = 9.17_5 \pm 0.29$  kcal/mol. However, a detailed analysis of the discussion accompanying the OH table in the JANAF Tables<sup>3</sup> leads to the conclusion that the value given by Gurvich et al.<sup>1</sup> should be preferred, since it appears to be based on more accurate and complete spectroscopic measurements. Namely, the JANAF tables<sup>3</sup> failed to consider the work of Carlone and Dalby.<sup>15</sup> Instead, they refer to the older (and longer, hence, inherently less precise) extrapolation of the same  $\text{A}^2\Sigma^+$  state of OH by Barrow<sup>16</sup> that produced  $D_0(\text{OH}) = 35450 \pm 100$  cm<sup>-1</sup>. Further inspection reveals that the actual extrapolated value<sup>16</sup> was 35427 cm<sup>-1</sup>, very close to the newer value of 35420  $\pm$  15 cm<sup>-1</sup> by Carlone and Dalby,<sup>15</sup> which Barrow increased in the final analysis to 35450  $\pm$  100 cm<sup>-1</sup> to compensate for a suspected underestimate. In the discussion of how the OH values were obtained, the

JANAF Tables<sup>3</sup> explicitly list the latter value as the adopted  $D_0(\text{OH})$ , together with  $\Delta H_{f0}^\circ(\text{OH}) = 9.26 \pm 0.29$  kcal/mol, which correctly results from such selection.<sup>17</sup> Inexplicably, the actual value listed on top of the OH page in the JANAF tables and used in the tabulated thermodynamic functions is different:  $\Delta H_{f0}^\circ(\text{OH}) = 9.17_5 \pm 0.29$  kcal/mol. Because this corresponds very closely to  $D_0(\text{OH}) = 35480 \pm 100$  cm<sup>-1</sup>, it is not clear whether the discrepancy is another *lapsus*<sup>18</sup> or the authors had some undisclosed reasons to additionally increase Barrow's<sup>16</sup> estimated  $D_0(\text{OH})$  by 30 cm<sup>-1</sup>. The latest NIST-JANAF tables<sup>19</sup> do not introduce any changes regarding OH and hence still neither consider Carlone and Dalby<sup>15</sup> nor shed any light on the curious discrepancy between the discussed and selected values. Taking all of the above into account, one concludes that the best available experimental spectroscopic evidence suggests  $D_0(\text{OH}) = 35420 \pm 15$  cm<sup>-1</sup> ( $= 101.271 \pm 0.04_3$  kcal/mol), and consequently  $D_0(\text{H-OH}) = \Delta H_{\text{atomiz0}}^\circ(\text{H}_2\text{O}) - D_0(\text{OH}) = 118.08_4 \pm 0.04_9$  kcal/mol  $= 41301 \pm 17$  cm<sup>-1</sup>.

In contrast to the approach through  $D_0(\text{OH})$  and  $\Delta H_{\text{atomiz0}}^\circ(\text{H}_2\text{O})$ , the positive ion cycle offers an independent and more direct route to  $D_0(\text{H-OH})$ . The positive ion thermochemical cycle is frequently utilized within the framework of a general approach that extracts accurate and reliable bond dissociation energies from photoionization and photoelectron measurements.<sup>14,20</sup> The problem at hand involves the enthalpies of reaction for the following two processes:



$\Delta H_{f0}^\circ(4)$  corresponds to the 0 K appearance energy of the  $\text{OH}^+$  fragment from water,  $\text{AE}_0(\text{OH}^+/\text{H}_2\text{O})$ , and can be obtained from photoionization mass spectrometric (PIMS) measurements.  $\Delta H_{f0}^\circ(5)$  is the adiabatic ionization energy of OH,  $\text{IE}(\text{OH})$ , and can be measured either by photoionization (PI) or photoelectron (PE) spectroscopy.<sup>21</sup> The thermochemical cycle is closed by applying  $\Delta H_{f0}^\circ(4) - \Delta H_{f0}^\circ(5) = \Delta H_{f0}^\circ(1)$ , and hence,  $D_0(\text{H-OH}) = \text{AE}_0(\text{OH}^+/\text{H}_2\text{O}) - \text{IE}(\text{OH})$ .

The photoionization appearance energy of the  $\text{OH}^+$  fragment from water was first reported by Dibeler et al.<sup>22</sup> as a "sharp onset" at  $\sim 18.05$  eV. This value was extracted from a rather coarse spectrum and does not contain the necessary correction for the internal energy of water. Subsequently, McCulloh<sup>23</sup> performed a very detailed photoionization study on  $\text{H}_2\text{O}$  and  $\text{D}_2\text{O}$ . For  $\text{H}_2\text{O}$ , he reported the 0 K fragmentation onset of  $18.115 \pm 0.008$  eV.

The adiabatic ionization energy (IE) of OH has a slightly more colorful history. The often referenced early photoionization values, such as 12.94 eV by Dibeler et al.,<sup>22</sup> 12.88 eV by Berkowitz et al.,<sup>24</sup> and 13.00 eV by McCulloh,<sup>23</sup> are actually indirect and depend, among others, on auxiliary thermochemical values,<sup>25</sup> including  $\Delta H_{f0}^\circ(\text{OH})$ . Subsequent direct photoelectron studies of IE of  $\text{OH}^{26-29}$  reported 13.01 eV. So far, the most accurate adiabatic ionization energy of OH has been reported in a zero kinetic energy photoionization (ZEKE) study<sup>30</sup> as  $104989 \pm 2$  cm<sup>-1</sup>  $\equiv 13.01698 \pm 0.00025$  eV. It should be noted that, as opposed to these photoelectron and ZEKE studies, direct photoionization mass spectrometry of the OH radical<sup>31-33</sup> produces an  $\text{OH}^+$  signal at energies that are slightly lower than the adiabatic  $\text{IE}(\text{OH})$ . However, this appears to be entirely attributable to rotational hot bands.<sup>32,33</sup>

Taking the best available literature values<sup>23,30</sup> to complete the positive ion cycle, namely,  $\text{AE}_0(\text{OH}^+/\text{H}_2\text{O}) = 18.115 \pm 0.008$  eV and  $\text{IE}(\text{OH}) = 13.0170 \pm 0.0003$  eV, results in  $D_0(\text{H-OH}) = 117.56 \pm 0.18$  kcal/mol  $= 41118 \pm 65$  cm<sup>-1</sup>, which is noticeably (0.52 kcal/mol or  $\sim 180$  cm<sup>-1</sup>) lower than the recommended value, as pointed out by Berkowitz et al.<sup>14,34</sup> In other words, the sum of the two independently determined values for the successive O-H bond dissociation energies in water, where  $D_0(\text{H-OH})$  is from the positive ion cycle and  $D_0(\text{OH})$  is from Carlone and Dalby,<sup>15</sup> produces  $218.83 \pm 0.19$  kcal/mol, which is at variance with  $\Delta H_{\text{atomiz0}}^\circ(\text{H}_2\text{O}) = 219.35_5 \pm 0.02_4$  kcal/mol by more than twice the collective error bar. Consequently, at least one of the following must be true:

(1)  $\Delta H_{\text{atomiz0}}^\circ(\text{H}_2\text{O})$ , as implied by generally accepted values<sup>1,2,3</sup> for  $\Delta H_{f0}^\circ(\text{H}_2\text{O})$ ,  $\Delta H_{f0}^\circ(\text{H})$ , and  $\Delta H_{f0}^\circ(\text{O})$  is too high;

(2)  $D_0(\text{OH})$  of Carlone and Dalby<sup>15</sup> is too low;

(3)  $D_0(\text{H-OH})$  as obtained from the positive ion cycle is too low.

It is fair to state that hypothesis 1 does not appear to be likely at all and is submitted here only for the sake of completeness of argument. The relevant thermochemical quantities,  $\Delta H_{f298}^\circ(\text{H}_2\text{O})$ ,  $\Delta H_{f298}^\circ(\text{H})$ , and  $\Delta H_{f298}^\circ(\text{O})$ , are the pillars of any serious thermodynamical compilation, and one would like to believe that they have been extremely carefully examined more than once and, if nothing else, implicitly validated through constant use. A scrutiny of the underlying measurements<sup>4-7</sup> suggests that these belong to a small select group of very meticulous thermochemical determinations. Hence, we have proceeded by assuming that  $\Delta H_{\text{atomiz0}}^\circ(\text{H}_2\text{O})$  is correct.

Hypothesis 2, however, would be much less surprising. Birge-Sponer extrapolations<sup>35</sup> are notorious for inaccuracies,<sup>36,37</sup> particularly when excited electronic states are used. They rely on the assumption that  $\Delta G(v + 1/2)$  for the unobserved levels, all of the way up to the dissociation limit, can be safely extrapolated from a polynomial fit of the observed  $\Delta G(v + 1/2)$  terms. The usual polynomial fit is inherently equivalent to a Dunham<sup>38</sup> expansion of the potential about the equilibrium distance, which typically gives a very reasonable representation of the vibrational levels deep in the potential well, but is intrinsically a poor approximation close to the dissociation limit.<sup>39</sup> In case of hydroxyl, the apparently convincing counterargument is that the extrapolations for both OH and OD are rather short ( $\sim 1.5$  vibrational levels) and that the isotopic difference between the derived dissociation energies is close to the expected value.<sup>15,40</sup> The selected value for  $D_0(\text{OH})$  seems to be further corroborated by observed broadening of rotational lines in OH and OD, attributed to predissociation.<sup>15,40</sup>

Hypothesis 3, which has been tacitly assumed to be the source of the inconsistencies,<sup>14,34</sup> can be further partitioned into:

(3a)  $\text{IE}(\text{OH})$  is too high;

(3b)  $\text{AE}_0(\text{OH}^+/\text{H}_2\text{O})$  is too low.

Hypothesis 3a is not particularly likely. Admittedly, the inherent lack of mass selection causes the ionization threshold region of OH to be congested in all photoelectron studies<sup>26-29</sup> by peaks from other species present during production of OH, such as  $\text{H}_2\text{O}$ ,  $\text{O}_2$ , H, and even HOF, and the final OH spectrum has to be obtained by some form of subtraction of these impurities. However, the Franck Condon factors for the  $\text{OH}^+ X^3\Sigma^- \leftarrow \text{OH } X^2\Pi_{3/2}$  transition favor the  $0 \leftarrow 0$  vibrational peak, which appears to be clearly visible in all studies, with the  $1 \leftarrow 0$  transition being much smaller (but still usually identifiable despite impurities). Consequently, it is highly improbable that the  $0 \leftarrow 0$  transition is misassigned and that the true adiabatic ionization onset is lower, because, to maintain a reasonable Franck-Condon envelope continuing with the two existing peaks, the hypothetically missing lower member of the progression would have to correspond to an even higher peak, clearly



absent in the spectra. Hence, the photoelectron value of  $\text{IE}(\text{OH}) = 13.01 \text{ eV}$  is not likely to be in error. In addition, ZEKE spectra<sup>30</sup> contain rotationally resolved information, which was successfully modeled theoretically, and hence serves as an effective fingerprint identifying both the species and the states that are involved. Finally, the ZEKE study reports that  $\text{IE}(\text{OD}) - \text{IE}(\text{OH}) = 96 \pm 3 \text{ cm}^{-1}$ . This can be compared with the difference of  $98.7 \text{ cm}^{-1}$  that can be obtained from zero-point vibrational energies (ZPE), Dunham corrections, and rotational term values.<sup>40</sup>

Finally, hypothesis 3b, although not at all impossible, would be quite unusual. Conventional wisdom has it that PIMS fragment appearance energies, *if properly extracted and corrected*, correspond technically to *strict upper limits*. Fragment onsets can be “retarded” by competitive or delayed fragmentation (“kinetic shift”), but apart from collisional and field effects (which can be avoided by careful experiments), it is difficult to see how a fragment might appear below its thermochemical threshold. Although onset retardation has been known to frustrate measurements in large molecules and/or higher fragmentation processes, it does not apply here, and even if it were applicable, it would mean that the actual thermochemical threshold is even lower, further escalating the discrepancy with the result of Carlone and Dalby. However, the key to obtaining an honest upper limit to the appearance energy is in the proper extraction of the threshold and correction for the effect(s) of internal energy. The typical shape of the PIMS fragmentation onset consists of an ascent in the fragment ion yield, preceded at lower energies by a long pseudoexponential “tail”.<sup>20,41</sup> The “tail” is related to the distribution of internal energies over the rotational and vibrational states of the starting neutral molecule and, hence, thermally dependent. The observed position of the ascent in the fragment ion yield curve is also thermally dependent, because it is shifted toward lower energy by an amount equal to the average internal energy present in the initial molecule. Traditionally, PIMS fragmentation onsets have been (and in most cases still are) derived by graphical extrapolation (linear or otherwise) of the observed ion yield ascent to the baseline, followed by a correction for the thermally dependent shift. The extrapolation is effectively an attempt to separate the actual ascent of the fragment ion yield from the “tail” region. Unfortunately, this approach suffers from a significant degree of subjectivity, although in good cases it can admittedly produce quite accurate fragment appearance energies. It should be noted, though, that, in the analysis of his PIMS spectra, McCulloh<sup>23</sup> introduced an additional (and quite unusual) step: he took the estimated 0 K fragment curve that he had obtained by graphically extrapolating the upper portion of the experimental fragment ion yield, convoluted it with the classical energy distributions for three rotational degrees of freedom, and compared it to the experimental data. Although the primary reason for the addition of this step was to demonstrate that *all* of the internal rotational energy is available for the fragmentation process (by fitting data at two different temperatures), it effectively introduced a secondary check on the extrapolated onset and, as such, is clearly superior to a simple one-step graphical extrapolation. However, careful as it seems, the procedure applied by McCulloh may still suffer from some degree of subjectivity hidden in the extrapolation step leading to the assumed 0 K fragmentation curve. In fact, a close examination of his analysis shows that the convoluted fragment curve slightly overestimates the “tail” region, suggesting that the reported  $\text{AE}_0(\text{OH}^+/\text{H}_2\text{O})$  may be slightly too low. Of course, the threshold reported by McCulloh may also have other, more

trivial sources of systematic errors, such as an inadvertent wavelength calibration error or peculiar experimental conditions causing undesired pressure or field effects, etc.

The discussion presented above suggests that a closer scrutiny of the experimental determinations underlying hypotheses 2 and 3b should shed light on the discrepancy surrounding  $\Delta H_{\text{r}0}^{\circ}(\text{OH})$ . In this paper, we examine hypothesis 3b by reinvestigating the  $\text{OH}^+$  fragment onset in the photoionization spectrum of water both by mass-selected photoionization (PIMS) of a thermally equilibrated sample and by pulsed-field-ionization photoelectron (PFI-PE) spectroscopy of a supersonically cooled sample. We also examine hypothesis 2 by analyzing and critiquing the Birge-Sponer extrapolation used by Carlone and Dalby.

While providing an independent check of possible systematic errors in the previous photoionization determination, the re-investigation by PIMS is also expected to provide a more robust value for  $\text{AE}_0(\text{OH}^+/\text{H}_2\text{O})$  than that obtained by McCulloh.<sup>23</sup> Namely, over the recent years, we have developed an approach for extracting fragment appearance energies that dispenses entirely with the extrapolation step.<sup>42</sup> This approach is based on direct numerical fitting of spectra with a model function that describes the fragment threshold region at the actual temperature of the experiment and includes both the fragment ascent and the asymptotic tail region. When the procedure produces a good fit, then the determined 0 K fragment appearance energy is very reliable and quite accurate.<sup>43</sup> On the other hand, an unsatisfactory fit clearly indicates that there is some complication associated with the threshold in question, and hence, it cannot be used straightforwardly for thermochemical purposes, a fact that can be quite difficult to obtain from graphical treatments.

High-resolution PFI-PE studies of small supersonically cooled molecules can produce a distinct steplike feature corresponding to the 0 K fragmentation onset, as recently shown by Weitzel et al.,<sup>44</sup> if the underlying fragmentation process fulfills certain conditions. The process is rather weak, but its observation became possible with the exceptional brilliance of third-generation synchrotrons. A disadvantage is that the PFI-PE approach inherently lacks mass selectivity, so that there is no guarantee that a particular spectral feature indeed corresponds to the formation of a fragment. A possible additional disadvantage is that the internal energy distribution of supersonically cooled molecules does not necessarily correspond to an equilibrated distribution defined by a single temperature. However, Weitzel et al. have shown that the step onset indeed corresponds to a 0 K value for  $\text{CH}_4$  and  $\text{C}_2\text{H}_2$ . Hence, when measurable, and particularly if it produces a value closely correlated to that which has been obtained by PIMS of a thermally equilibrated sample and/or by photoelectron-photoion coincidence (PEPICO) studies, the steplike onset provides additional confirmation for the fragmentation threshold in question.

Additional insights on the question of the correct value for  $\Delta H_{\text{r}0}^{\circ}(\text{OH})$  can be obtained from high-level theoretical computations. At the G2 level of theory,<sup>45</sup>  $\Delta H_{\text{r}0}^{\circ}(\text{OH}) = 9.0 \text{ kcal/mol}$ , whereas at the G3 level of theory,<sup>46</sup> this becomes  $8.4 \text{ kcal/mol}$ . Although vaguely suggestive of an enthalpy that is lower than the experimental value of Gurvich et al.,<sup>1</sup> these high-level calculations are not quite accurate enough<sup>47</sup> to distinguish discrepancies of the order of  $0.5 \text{ kcal/mol}$ . However, for a species of the size of OH or even  $\text{H}_2\text{O}$ , much more sophisticated calculations are now possible.

A composite theoretical approach to predict uniformly accurate thermochemical properties across a range of small-to-intermediate size chemical systems without recourse to empirical

correction parameters to the computed total electronic energy has been recently in development.<sup>48</sup> High-level ab initio electronic structure methods are used to calculate the molecular atomization energy. The energy of the valence electrons are calculated by using frozen-core (FC) coupled cluster methods including single, double, and connected triple excitations [CCSD(T)], with the latter being handled perturbatively.<sup>49</sup> The CCSD(T) energies are extrapolated to the complete basis set (CBS) limit, a step that is facilitated by the uniform convergence properties of the correlation consistent basis sets (cc-pVnZ) from Dunning and co-workers.<sup>50</sup> Core/valence corrections are obtained from CCSD(T) calculations by using the cc-pCVnZ basis sets which contain additional functions in the core electron region, and scalar relativistic corrections are obtained from CCSD(T)(FC)/unc-cc-pVnZ calculations. Further corrections to the atomization energy for higher order excitations are based on full configuration interaction (FCI) computations. This procedure leads to total electronic energies that are entirely computational and do not incorporate any experimental corrections. Atomization energies are obtained from these total electronic energies by adding either experimental or calculated zero-point vibrational energies for the molecular species and subtracting computed total electronic energies of the atoms. These atomization energies refer to the weighted average of the available spin multiplets of the molecular and atomic species and are, where necessary, further corrected by incorporating experimental spin-orbit splittings. The atomization energies computed and corrected in this manner can then be directly compared to atomization energies obtained from experimental enthalpies of formation. Alternatively, the computed atomization energies can be expressed as enthalpies of formation with the aid of experimental atomic heats of formation. The accuracy of the computed atomization energies is essentially limited by the size of the species and the computational resources available (which limit the highest  $\zeta$ -order of the basis set than can be used). For OH and H<sub>2</sub>O, the achievable accuracy is expected to be of the order of 0.2–0.3 kcal/mol, and hence, theory should be capable of distinguishing between the two competing experimental values that are discussed above.

## 2. Experimental Results and Discussion

Two different experimental setups were used in present experiments: one at Argonne National Laboratory (PIMS experiments) and the other at Lawrence Berkeley National Laboratory (PFI-PE and PEPICO experiments). The results of each are described in turn.

**2.1. PIMS Studies.** The basic instrumental setup at Argonne, employed in the present PIMS studies, was recently described elsewhere.<sup>51</sup> The light source is a discharge lamp, followed by a 3 m vacuum-ultraviolet normal-incidence monochromator that is mated to the main vacuum chamber. The main chamber has provisions for measuring ions that are mass-selected by a quadrupole filter, near-zero energy electrons, and light intensity and is outfitted with various in situ sources of radicals. The experiments described here used the helium Hopfield emission continuum. The mass-selected ions were pulse-counted, whereas the light intensity was monitored via fluorescence of a sodium-salicylate-coated window coupled to an external photomultiplier. The response of the sodium-salicylate transducer was assumed to be wavelength independent in the region of interest. The nominal photon resolution was kept at 0.08 nm (fwhm), and the spectra were scanned at a constant 0.02 nm step size. The small atomic emission lines of Ne i, N ii, and H i superimposed

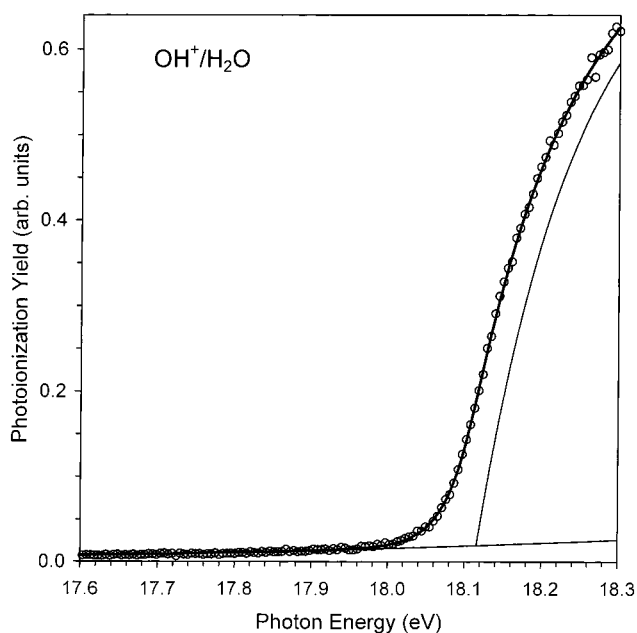


**Figure 1.** Photoion yield curve of the OH<sup>+</sup> fragment from water in the vicinity of the threshold region obtained in the present PIMS experiments on a thermally equilibrated (25 °C) H<sub>2</sub>O sample. The solid line passing through the points is a model fit incorporating the effect of the internal energy distribution of water, whereas the line displaced toward higher energy is the derived fragment yield at 0 K. The general appearance of the threshold and the quality of the fit demonstrate that the onset conforms to a well-behaved photodissociative ionization process. The best fitted threshold using the discrete distribution of internal energies and including the resolution effect is  $Ae_0(\text{OH}^+/\text{H}_2\text{O}) = 18.116_1 \pm 0.003_5$  eV.

on the continuum served as accurate wavelength calibration markers. In particular, all scans were extended to include the Ne i lines. The absolute wavelength calibration of the present PIMS experiments is believed to be accurate to slightly better than 0.01 nm (or  $<1/2$  step size).

Figure 1 displays the photoion yield curve of the OH<sup>+</sup> fragment from water in the vicinity of the threshold region obtained in the present PIMS experiments on a thermally equilibrated (25 °C) H<sub>2</sub>O sample. The general appearance of the onset conforms to the expected shape of the photoion yield curve that corresponds to a well-behaved photodissociative ionization process.

Possible complications arising from collisional effects are most easily discerned in the tail region preceding the onset, where, if present, the ion signal will show a nonlinear dependence on sample pressure. We have checked explicitly for this behavior and verified that at the sample pressures utilized in the present experiments the response of the ion signal was linear. Checking explicitly for the effect of the repeller field in the ionization region is somewhat less straightforward, because this setting cannot be changed by substantial amounts independently of the other ion optics. For these measurements, the repeller field was explored within the range of our usual setting ( $\sim 2$ – $3$  V/cm), and the other lenses were optimized accordingly. No changes in the threshold shape were observed, consistent with our extensive past experience that strongly suggests that at these values the field effect on the fragmentation threshold is negligible. Hence, to the best of available evidence, the spectrum in Figure 1 is devoid of significant field and collisional effects.

The solid line passing through the data in Figure 1 is a least-squares fit with a threshold model function. The overall quality

of the fit in Figure 1 appears to be excellent, clearly suggesting that the underlying fragmentation process is well behaved. The procedure for obtaining appearance energies by fitting experimental ion yield curves with model functions was described in greater detail previously.<sup>42</sup> The function that was used to fit the experimental data consisted of a kernel function, which was convoluted with a second function describing the vibrational and rotational energy distribution of the starting water molecule at the temperature of the experiment. The underlying ion background level was predetermined in separate fits, which were restricted to points at wavelengths significantly longer than the examined threshold. Several different backgrounds were used, including two limiting extremes in which the background level was slightly (but noticeably) underestimated or overestimated. The kernel function used in the present case had the usual form of  $\{1 - \exp[-\beta(h\nu - AE_0)]\}$ , where  $h\nu$  is the photon energy,  $AE_0$  is the 0 K fragmentation threshold, and parameter  $\beta$  adjusts the shape of the kernel function such that it can reproduce the slowing down in the growth of the fragment ion yield toward higher energy.

Aside from the desired appearance energy  $AE_0$ , the only free parameters of the fit were  $\beta$  (curvature at higher energy) and a scalar factor that adjusts the fitting function to the relative ion yield of the experiment. Besides using several differing backgrounds, the actual fitting of data was performed using four different representations for the internal energy distribution, each corresponding to a successively higher level of sophistication. Meticulous direct state counting<sup>1,2</sup> (including vibrational anharmonicity, Darling–Denison resonance, rigid rotator with the Stripp–Kirkwood correction factor, and corrections for centrifugal distortion) produces a rotational and vibrational internal energy  $\langle E \rangle_{\text{vib,rot}}$  of water of 1.495<sub>6</sub> kT at 298.15 K (0.03842<sub>6</sub> ± 0.00005<sub>2</sub> eV or 309.9<sub>3</sub> ± 0.4<sub>2</sub> cm<sup>-1</sup>). We have rechecked this quantity by using a discrete state count that implicitly includes all of these (and any other) corrections, because it is based on the best currently available list of rovibrational levels of the ground state of H<sub>2</sub>O.<sup>52,53</sup> This produces a practically identical value of 1.495<sub>2</sub> kT at 298.15 K (0.03841<sub>7</sub> eV or 309.8<sub>5</sub> cm<sup>-1</sup>). Because the dominant contribution to  $\langle E \rangle_{\text{vib,rot}}$  are rotations and the accurately calculated value differs from 1.5 kT by <1 cm<sup>-1</sup>, the distribution of the internal energy can be expected to be quite close to that corresponding classically to three degrees of rotation,  $E^{1/2} \exp(-E/kT)$ . This representation, which was also the basis for McCulloh's<sup>23</sup> analysis, corresponds to the simplest form of the internal energy distribution used in the present fits. The next two levels of sophistication in the representation of the internal energy distribution were both based on the analytical form  $E^\eta \exp(-\alpha E)$ , where  $\alpha$  is slightly adjusted so that  $\langle E \rangle_{\text{vib,rot}} = 1.495_6$  kT.<sup>54</sup> In one case,  $\eta$  was kept at 0.5, and in the other, the “best”  $\eta$  was determined by fitting the discrete distribution of internal energies cited above.<sup>55,56</sup> Finally, we also performed a least-squares fit of the data using a model function that was based on numerical convolution of the kernel function with the discrete distribution of vibrational and rotational energies.

With the simplest form for the internal energy distribution function,  $E^{1/2} \exp(-E/kT)$ , the fitted values clustered very closely around 18.115<sub>3</sub> eV, with a spread of ±0.001<sub>1</sub> eV that arises primarily from the uncertainty in the underlying background. Increasing the error bar to reflect other uncertainties (including those related to the wavelength scale calibration) leads to  $AE_0(\text{OH}^+/\text{H}_2\text{O}) = 18.115_3 \pm 0.003_5$  eV. This result should be directly comparable to that obtained by McCulloh (18.115 ± 0.008 eV). Clearly, the two are in superb agreement.

Proceeding to fits with more sophisticated representations of the internal energy distribution of H<sub>2</sub>O, one finds that, for a given choice of background, the fitted values for  $AE_0$  are essentially independent (within a span of <0.2 meV) on the particular choice for the internal energy distribution function. In fact, using the more sophisticated representations leads to fitted values that differ mutually by negligible amounts but are systematically lower by ~0.1 meV than those obtained with the simplest representation. The only other noticeable effect of using successively more sophisticated representations for the internal energy distribution was a slight, but consistent, improvement in the  $\chi^2$  of the fit. Any of the fits mentioned so far do not explicitly take into account the effect of instrumental resolution, which for a featureless fragment ion curve such as the present one is very small and can be ordinarily ignored.<sup>57</sup> However, in the present case, we have repeated all fits by including explicitly the resolution effect and found that this produces thresholds that are consistently 0.9 meV higher, further systematically reducing the  $\chi^2$ . Taking all of the above into account, the best fitted threshold using the discrete distribution of internal energies and including the resolution effect is  $AE_0(\text{OH}^+/\text{H}_2\text{O}) = 18.116_1 \pm 0.003_5$  eV (= 146116 ± 28 cm<sup>-1</sup>).

**2.2. PFI–PE and PEPICO Studies.** The PFI–PE and PEPICO studies presented here were conducted at the Advanced Light Source at Lawrence Berkeley National Laboratory, utilizing the high-resolution monochromatized VUV source of the Chemical Dynamics Beamline. The setup of the Beamline and its capabilities have been described<sup>58,59</sup> in detail elsewhere. The procedures for PFI–PE measurements using the photoelectron-photoion facility of the Chemical Dynamics Beamline have been also described previously.<sup>60</sup> Briefly, the gaseous sample (H<sub>2</sub>O in this case) is introduced into the photoionization/photoexcitation (PI/PEX) region of the apparatus as a skimmed supersonic beam, achieving a temperature of ~30 K.<sup>61</sup> Each 656 ns period of the ALS light pattern in the normal multibunch operation consists of 256 light pulses (50 ps each, separated by 2 ns) and a dark gap of 144 ns. Excited parent species in high- $n$  ( $n > 100$ ) Rydberg states, formed by excitation of the beam sample at the PI/PEX center by the dispersed synchrotron radiation, are field ionized by an electric field pulse (1.5 V/cm, 40 ns) applied during the dark gap and delayed by 20 ns with respect to the beginning of the dark gap. Electrons formed by PFI in the dark gap are selected by a time-of-flight scheme using a detection time gate. The photon energy calibration was achieved using rare gas PFI–PE bands recorded under the same experimental conditions. Previous experiments indicate that the accuracy of this calibration method is within ±0.5 meV.<sup>58,59,62</sup>

Figure 2 depicts the PFI–PE spectrum of supersonically cooled water in the vicinity of the expected OH<sup>+</sup> threshold. The distinct steplike feature at ~18.115 eV almost certainly corresponds to the desired onset. Previous comparisons<sup>44</sup> of the PFI–PE steplike features in CH<sub>4</sub>, corresponding to the onset of CH<sub>3</sub><sup>+</sup> fragment, and C<sub>2</sub>H<sub>2</sub>, corresponding to C<sub>2</sub>H<sup>+</sup> fragment, with PFI–PEPICO breakdown diagrams indicate that the desired onset is located close to the point where the step levels off. The actual apex of the step in Figure 2, which would then correspond to an upper limit to  $AE_0(\text{OH}^+/\text{H}_2\text{O})$ , occurs at 18.116<sub>5</sub> ± 0.002<sub>0</sub> eV (= 146119 ± 16 cm<sup>-1</sup>), lending full support to the mass-analyzed fragmentation threshold obtained above.

Additional support for these values can be gleaned from the breakdown diagram obtained in PEPICO experiments (Figure 3). The disappearance point of the parent, which currently appears to be the best way to recover the desired thermochem-



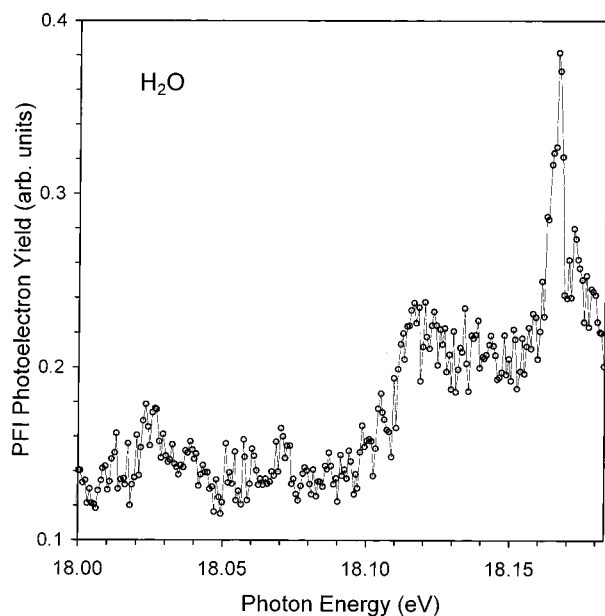


**Figure 2.** PFI-PE spectrum of supersonically cooled water in the vicinity of the expected  $\text{OH}^+$  threshold. The distinct steplike feature at  $\sim 18.115$  eV almost certainly corresponds to the desired onset. The apex of the step, which corresponds to an upper limit to  $\text{AE}_0(\text{OH}^+/\text{H}_2\text{O})$ , occurs at  $18.116_5 \pm 0.002_0$  eV.

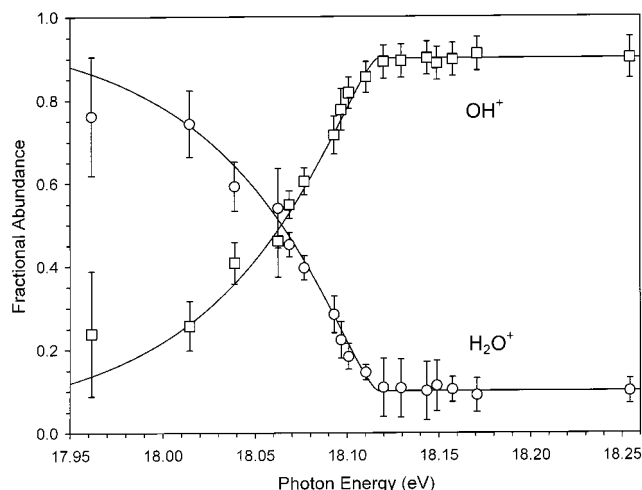


**Figure 3.** Breakdown diagram for  $\text{H}_2\text{O} \rightarrow \text{H} + \text{OH}^+ + \text{e}^-$  obtained in PEPICO experiments. The lines are intended only to guide the eye and do not affect the determination of the disappearance point of the parent, which corresponds to  $\text{AE}_0(\text{OH}^+/\text{H}_2\text{O})$  and occurs at  $18.115 \pm 0.005$  eV.

istry from a breakdown diagram,<sup>44</sup> occurs at  $18.115 \pm 0.005$  eV ( $= 146107 \pm 40 \text{ cm}^{-1}$ ).

**2.3. Discussion of Experimental Results.** The very good agreement between four completely separate determinations of the fragmentation onset of  $\text{OH}^+$  from  $\text{H}_2\text{O}$  (one from the literature and three presented here) has a synergistic effect and quite strongly suggest that the experimental values are not biased by systematic errors arising from peculiar experimental conditions, instrumental effects, or human errors, such as pressure and field effects, wavelength calibration problems, or inappropriate threshold interpretation. Furthermore, the fact that PFI-PE studies of supersonically cooled samples (which measure near-zero energy electrons) produce the same result as PIMS studies of thermally equilibrated samples, further restricts the hypothetical range of systematic errors that could be construed by postulating various peculiarities of the underly-

ing fragmentation process. Hence, we conclude that the fragmentation threshold, as determined by photoionization experiments, corresponds with extremely high probability to the thermodynamically correct onset.

Combining the 0 K appearance energy determined from our PIMS studies of  $146116 \pm 28 \text{ cm}^{-1}$  ( $18.116_1 \pm 0.003_5$  eV) with the best available adiabatic ionization energy<sup>30</sup> of OH,  $104989 \pm 2 \text{ cm}^{-1}$ , results in  $D_0(\text{H}-\text{OH}) = 41127 \pm 28 \text{ cm}^{-1} = 117.59 \pm 0.08 \text{ kcal/mol}$ , implying  $D_0(\text{OH}) = 35594 \pm 29 \text{ cm}^{-1} = 101.77 \pm 0.08 \text{ kcal/mol}$  and  $\Delta H_{f0}(\text{OH}) = 8.85 \pm 0.08 \text{ kcal/mol}$  (see Table 1 for these and following values). The PFI-PE step-onset of  $146119 \pm 16 \text{ cm}^{-1}$  leads to very similar values of  $D_0(\text{H}-\text{OH}) = 41130 \pm 16 \text{ cm}^{-1} = 117.60 \pm 0.05 \text{ kcal/mol}$ ,  $D_0(\text{OH}) = 35590 \pm 18 \text{ cm}^{-1} = 101.76 \pm 0.05 \text{ kcal/mol}$ , and  $\Delta H_{f0}(\text{OH}) = 8.86 \pm 0.05 \text{ kcal/mol}$ . Finally, the coarser value from the breakdown diagram,  $146107 \pm 40 \text{ cm}^{-1}$  (which is, aside from the smaller error bar, identical to the value of McCulloh<sup>23</sup>), results in  $D_0(\text{H}-\text{OH}) = 41118 \pm 40 \text{ cm}^{-1} = 117.56 \pm 0.12 \text{ kcal/mol}$ , implying  $D_0(\text{OH}) = 35602 \pm 41 \text{ cm}^{-1} = 101.79 \pm 0.12 \text{ kcal/mol}$  and  $\Delta H_{f0}(\text{OH}) = 8.83 \pm 0.12 \text{ kcal/mol}$ .

A weighted average of these three very slightly differing sets of values, obtained by minimizing  $\chi^2$ , produces  $\text{AE}_0(\text{OH}^+/\text{H}_2\text{O}) = 146117 \pm 24 \text{ cm}^{-1}$  ( $18.116_3 \pm 0.003_0$  eV) and  $D_0(\text{H}-\text{OH}) = 41128 \pm 24 \text{ cm}^{-1} = 117.59 \pm 0.07 \text{ kcal/mol}$ , corresponding to  $D_0(\text{OH}) = 35593 \pm 25 \text{ cm}^{-1} = 101.76 \pm 0.07 \text{ kcal/mol}$  and  $\Delta H_{f0}(\text{OH}) = 8.85 \pm 0.07 \text{ kcal/mol}$ . These are our currently recommended values on the basis of the positive ion cycle.

As we were preparing this manuscript, a study of photodissociation of  $\text{H}_2\text{O}$  at 121.6 nm by Harich et al.<sup>63</sup> appeared, reporting  $D_0(\text{H}-\text{OH}) = 41151 \pm 5 \text{ cm}^{-1} = 117.66 \pm 0.01 \text{ kcal/mol}$ . This value is in quite good agreement with the photoionization measurements reported here and certainly adds significant weight to the arguments made in the present study. However, on a finer scale of comparisons, it seems that this value is slightly ( $\sim 20 \text{ cm}^{-1}$  or  $\sim 0.06 \text{ kcal/mol}$ ) higher than the photoionization values discussed above. The reason for this very slight discrepancy is not quite clear. From  $\text{AE}_0(\text{OH}^+/\text{H}_2\text{O}) = D_0(\text{H}-\text{OH}) + \text{IE}(\text{OH})$ , the result by Harich et al. would imply that the 0 K appearance energy of  $\text{OH}^+$  from water is  $146140 \pm 5 \text{ cm}^{-1}$  ( $18.119_1 \pm 0.000_7$  eV). This seems to be in agreement with the result of McCulloh,  $18.115 \pm 0.008$  eV and the coincidence result presented here,  $18.115 \pm 0.005$  eV, which are the two photoionization measurements with the coarsest error bars but is only in marginal agreement with our PIMS threshold of  $18.116_1 \pm 0.003_5$  eV and just outside the error bar of our PFI-PE step-onset of  $18.116_5 \pm 0.002_0$  eV. One could argue that the latter corresponds to ionization not from the  $0_{00}$  (using  $J_{\text{KaKc}}$  notation) rotational ground state of  $\text{H}_2\text{O}$  but from the  $1_{01}$  level ( $23.8 \text{ cm}^{-1}$  above the  $0_{00}$  level), which is the lowest accessible level of ortho  $\text{H}_2\text{O}$  and in an ortho-para mixture is populated more than the  $0_{00}$  level even at the lowest temperatures. Although this interpretation has its undeniable appeal, the criticism is not applicable to the PIMS experiment, which was conducted at room temperature, particularly because the discrete distribution of internal energies used in its interpretation correctly takes into account the underlying 1:3 statistical weights of para and ortho  $\text{H}_2\text{O}$ . An entirely different possibility is that the ZEKE  $\text{IE}(\text{OH})$ , which is a common denominator in all four positive ion cycles discussed so far, is slightly too high. Although it would be quite surprising that the wavelength scale determination in the ZEKE experiment is off by as much as  $20 \text{ cm}^{-1}$ , the possibility is not entirely without merit, given the fact that all other photoelectron experiments report 13.01 eV

but none report 13.02 eV, which would be slightly more in line with the ZEKE determination. Finally, it could be argued that the measurement of Harich et al. depends critically on the accuracy with which the kinetic energy release is determined, which in turn depends on such factors as the geometrical accuracy of their instrumental setup.

Although the curious discrepancy between the current photoionization result and the value of Harich et al. merits additional investigation, it should be clearly recognized that its magnitude is largely inconsequential from the thermochemical point of view. Hence, we take the pragmatic approach and adopt as the experimentally recommended value the consensus of photoionization experiments,  $D_0(\text{H}-\text{OH}) = 41128 \pm 24 \text{ cm}^{-1}$ , particularly because its error bar, while still very small from the thermochemical point of view, allows for a sufficient overlap with the result of Harich et al.

### 3. Analysis of the Spectroscopic Determination of $D_0(\text{OH})$

In this section, the analysis of spectroscopic determination of  $D_0(\text{OH})$  will proceed in three steps. First we will describe in detail the work of Carlone and Dalby<sup>15</sup> responsible for that determination. Second, we will technically improve on their data reduction in small ways that together act to raise the derived value of  $D_0(\text{OH})$ . Third, we will supplement the data used by Carlone and Dalby by an ab initio electronic structure calculation.

Carlone and Dalby<sup>15</sup> have performed high-resolution measurements of the  $\text{B}^2\Sigma^+ \rightarrow \text{A}^2\Sigma^+$  and  $\text{C}^2\Sigma^+ \rightarrow \text{A}^2\Sigma^+$  band systems in OH, improving upon previous observations by Barrow.<sup>16</sup> From combination differences between corresponding lines of two bands having the same upper state, they obtained  $\Delta G(v + 1/2)$  values for  $\text{A}^2\Sigma^+$ ,  $(v + 1/2) = 0.5\text{--}8.5$  in OH and  $0.5\text{--}2.5$ ,  $6.5\text{--}12.5$  in OD.<sup>64</sup> A standard Birge–Sponer extrapolation, using the expression

$$\Delta G(v + 1/2) = \sum a_k(v + 1/2)^k; \quad k = 0, 1, \dots, n \quad (6)$$

with polynomials of orders  $n = 4, 5$ , or  $6$  produced an average  $(v + 1/2)_{\text{intercept}}$  of  $9.955$  for OH and  $13.836$  for OD. Integrals under the fitted  $\Delta G(v + 1/2)$  curves from  $0$  to  $(v + 1/2)_{\text{intercept}}$  yielded (with a relatively small dispersion,  $+7_{-4} \text{ cm}^{-1}$  for OH and  $+1_{-3} \text{ cm}^{-1}$  for OD) the values  $D_0(\text{OH}, \text{A}^2\Sigma^+) = 18847 \text{ cm}^{-1}$  (corresponding to an arithmetic average of the three fits) and  $D_0(\text{OD}, \text{A}^2\Sigma^+) = 19263 \text{ cm}^{-1}$  ( $2 \text{ cm}^{-1}$  higher than the average,  $19261 \text{ cm}^{-1}$ ). These  $D_0$  values refer to the H(or D)( $^2\text{S}$ ) + O( $^1\text{D}_2$ ) limit. The desired dissociation energy of ground-state  $\text{X}^2\Pi_{3/2}$ ,  $J = 3/2$ ,  $v=0$  of OH producing H( $^2\text{S}$ ) + O( $^3\text{P}_2$ ) was obtained by adding the energy<sup>65</sup> of the  $\text{P}_1(1)$  transition of  $32440.6 \text{ cm}^{-1}$  to  $D_0(\text{OH}, \text{A}^2\Sigma^+)$  and subtracting the term value<sup>66</sup> for O( $^1\text{D}_2$ ) of  $15867.7 \text{ cm}^{-1}$ , producing  $D_0(\text{OH}) = 35419.9 \text{ cm}^{-1}$ . Instead of deriving  $D_0(\text{OD})$  in an equivalent manner and comparing it to  $D_0(\text{OH})$  via the corresponding ZPEs of the X state, and/or comparing  $D_0(\text{OH}, \text{A}^2\Sigma^+)$  and  $D_0(\text{OD}, \text{A}^2\Sigma^+)$  via the ZPEs of the A state, Carlone and Dalby present a somewhat circuitous comparison,<sup>67</sup> leading to a residual difference of  $-5.8 \text{ cm}^{-1}$  (OD being more bound), which they attribute to *electronic* isotope shifts. However, because of a failure to properly account for all spectroscopic terms,<sup>67</sup> the residual difference actually is  $9.6 \text{ cm}^{-1}$  with OH being more bound. This change in sign may correspond to a somewhat less satisfactory result.<sup>68</sup>

Carlone and Dalby<sup>15</sup> attempt to find further support for the value  $D_0(\text{OH}) = 35419.9 \text{ cm}^{-1}$  by examining the observed predissociation patterns in OH and OD. Two different kinds of

predissociation are involved here. One kind refers to predissociation of higher levels of the A state via curve crossing, and the other refers to the highest rotational levels of the B state that are still contained within the potential well. The first manifests itself as broadened rotational lines, the second is inferred from the absence of lines. Predissociation via curve crossing affects levels of  $\text{A}^2\Sigma^+$  that are below its asymptotic H( $^2\text{S}$ ) + O( $^1\text{D}_2$ ) limit but above the H( $^2\text{S}$ ) + O( $^3\text{P}_2$ ) limit. The succinct picture that emerges from the more complete references given in Huber and Herzberg<sup>40</sup> is that predissociation in  $\text{A}^2\Sigma^+$  is observed for  $v=0$ ,  $N \geq 23$ ,  $v = 1$ ,  $N \geq 14$ , and all levels of  $v = 2$  in OH, and in OD  $v = 0, 1, 2$  and  $N \geq 29, 26, 17$ . The lowest-energy level, which sets an upper limit to the dissociation energy, is  $v = 2$  and  $N = 0$  of  $\text{A}^2\Sigma^+$  in OH. This is still  $2802 \text{ cm}^{-1}$  above the  $D_0(\text{OH})$  value of Carlone and Dalby<sup>15</sup> and, hence, not particularly useful.

In contrast to the above, predissociation by rotation in the  $\text{B}^2\Sigma^+$  state provides a better handle on the dissociation energy. This state has a shallow potential curve with an asymptotic limit H( $^2\text{S}$ ) + O( $^1\text{D}_2$ ) and an equilibrium internuclear distance that is nearly twice that of the X state.<sup>40</sup> The potential subtends only two vibrational levels in OH and three in OD.<sup>69</sup> Felenbok<sup>70</sup> first reported predissociation by rotation in this state, giving evidence that for OH the last rotational level in  $v = 0$  is  $N = 15$  and assuming that  $N = 8$  is the last level in  $v = 1$ . Although Carlone and Dalby<sup>15</sup> have observed  $N$  only up to  $10$  for  $v = 0$ , they observe transitions to  $N = 9$  of  $v = 1$ , one rotational quantum higher than Felenbok's surmise. The levels  $v = 0$  and  $N = 15$  and  $v = 1$  and  $N = 9$  can provide a lower limit to  $D_0(\text{OH}, \text{B}^2\Sigma^+)$  if the effect of the centrifugal barriers can be taken into account by, for example, constructing the appropriate limiting curves of dissociation. Similarly, if levels  $v = 0$  and  $N = 16$  and  $v = 1$  and  $N = 10$  indeed do not exist, they can provide an upper limit to the dissociation energy. In lieu of an estimated limiting curve of dissociation for  $\text{B}^2\Sigma^+$ , Carlone and Dalby use these four rotational levels<sup>71</sup> and straight lines on an  $N(N + 1)$  plot through two alternate pairs of levels to obtain estimates of the upper and lower limit to the dissociation energy, producing  $D_0(\text{OH}, \text{B}^2\Sigma^+) = 917 \pm 60 \text{ cm}^{-1}$ . Their analysis is reproduced in Figure 4. They also quote  $D_e(\text{OH}, \text{B}^2\Sigma^+) = 1355 \text{ cm}^{-1}$  inferred from the measured  $\Delta G(v+1/2)$  values for the B state of OH and OD, as well as a  $D_e$  of  $1360 \text{ cm}^{-1}$  from another limiting curve plot of the highest observed rotational levels in  $\text{B}^2\Sigma^+$  of OH. Although they do not explicitly give the ZPE value used or implied in their procedure, with a ZPE<sup>72</sup> of  $462.9 \text{ cm}^{-1}$ , these two  $D_e$  values correspond to  $D_0(\text{OH}, \text{B}^2\Sigma^+) = 892\text{--}897 \text{ cm}^{-1}$  in good agreement with  $917 \pm 60 \text{ cm}^{-1}$ . However, as noted by Carlone and Dalby, this result implies<sup>73</sup> values of  $D_0(\text{OH}, \text{A}^2\Sigma^+)$  of  $18943 \pm 30 \text{ cm}^{-1}$  or  $18965 \pm 60 \text{ cm}^{-1}$ , about  $100\text{--}120 \text{ cm}^{-1}$  higher than the value of  $18847 \pm 15 \text{ cm}^{-1}$  from the Birge–Sponer extrapolation on the A state. Carlone and Dalby argue that the shortness of the Birge–Sponer extrapolation makes the latter a more reliable estimate and conclude that the B state must have an inherent dispersion hump, i.e., a reverse dissociation barrier even at  $N = 0$ .

In the second step of our analysis, we will technically improve the Birge–Sponer study of the A state and the analysis of the predissociation of the B state. Consider first the Birge–Sponer extrapolation. We have repeated the fit of Carlone and Dalby (see Figure 5a) and obtained virtually identical results,<sup>74</sup> as long as the integrand was the fitted  $\Delta G(v + 1/2)$  function. For some reason Carlone and Dalby did not realize that the resulting  $D_0$  values are *lower* (by up to  $26 \text{ cm}^{-1}$ ) than the energy of the last (predicted) level,<sup>75</sup> as a direct consequence of the approximation



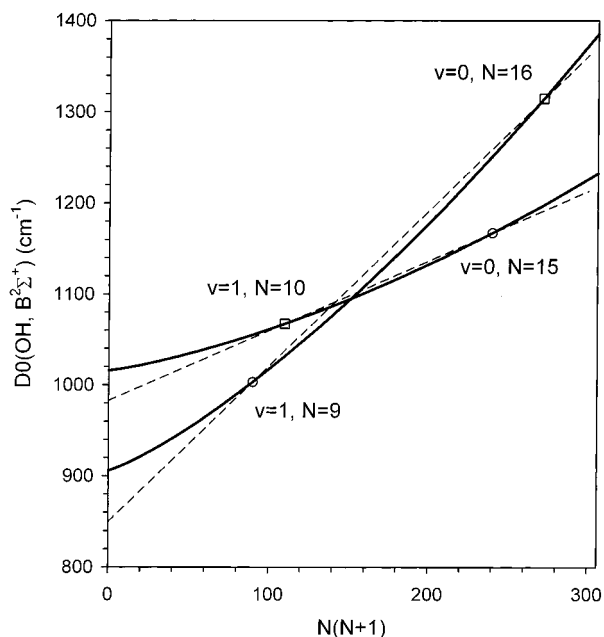


**Figure 4.** Limiting curves of dissociation of the  $B^2\Sigma^+$  state of OH. The circles correspond to the highest observed rotational levels,  $v = 0$  and  $N = 15$  and  $v = 1$  and  $N = 8$ . The  $N = 0$  intercept of the limiting curve (full line) passing through the last observed rotational state of  $v = 1$  and the first extrapolated rotational state of  $v = 0$  provides a lower limit to a plausible dissociation energy. Likewise, the limiting curve passing through the other pair of points provides an upper limit, bracketing  $D_0(\text{OH}, B^2\Sigma^+)$  to  $961 \pm 55 \text{ cm}^{-1}$ . The dashed straight lines correspond to the original simplified analysis in ref 15 which leads to an underestimate of  $D_0(\text{OH}, B^2\Sigma^+)$ .

$dG(v)/dv \approx \Delta G(v + 1/2)$ . The derivative  $d[G(v)]/dv$  can be obtained from the same data without much more effort,<sup>76</sup> producing slightly higher values<sup>77</sup>  $D_0(\text{OH}, A^2\Sigma^+) = 18866.7 \text{ cm}^{-1}$  and  $D_0(\text{OD}, A^2\Sigma^+) = 19272.3 \text{ cm}^{-1}$ , which represent the technically correct outcome that should have been obtained from a Birge–Spencer fit. The ZPE difference (including  $Y_{00}$  terms) based on the best available data<sup>40</sup> on the A state is  $420.8 \text{ cm}^{-1}$ , leading to a residual discrepancy of  $15.2 \text{ cm}^{-1}$ . Using the more convoluted approach of Carlone and Dalby<sup>67</sup> that relates the two  $D_0$  values through the ZPE differences of the ground electronic state produces  $19.6 \text{ cm}^{-1}$ . These shifts are slightly less convincing (certainly by size and perhaps by sign as well) than the original discrepancy of  $-5.8 \text{ cm}^{-1}$  quoted by Carlone and Dalby. Whether  $19.6$  and  $15.2 \text{ cm}^{-1}$  are plausible electronic isotope shifts of the X and the A state is an open question, which is very difficult to address without specialized calculations.<sup>78</sup>

Now consider predissociation in the B state. Although the underlying idea of pairing the four levels in a way that produces an upper and lower limit is excellent, the use of straight lines on an  $N(N + 1)$  plot implicitly leads to an underestimate of the dissociation energy. Figure 4 shows the straight lines of Carlone and Dalby, together with the more appropriate (albeit approximate) limiting curves of dissociation. These have been obtained from effective potential energy curves calculated by using

$$U_j(r) = U_0(r) + h/(8\pi^2 c \mu r^2) J(J + 1) \quad (7)$$

where  $J$  has been replaced by  $N$ , as appropriate for case b coupling and  $U_0(r)$  was approximated by a Morse curve.<sup>36</sup> For each  $N$ , the energy of the centrifugal maximum relative to the bottom of the Morse curve was converted to a scale relative to  $v = 0$  and  $N = 0$  by using a vibrational ZPE<sup>79</sup> of  $462.9 \text{ cm}^{-1}$ .

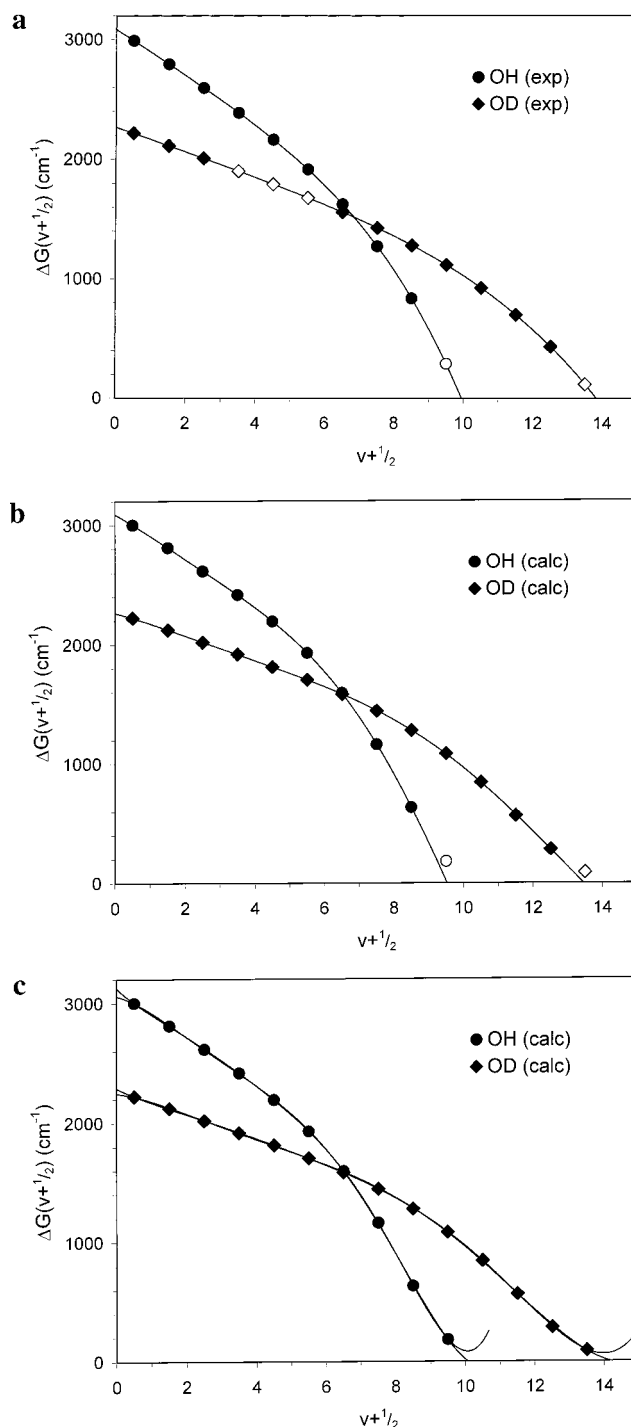


**Figure 5.** Birge–Spencer extrapolations of the vibrational gaps in the  $A^2\Sigma^+$  state of OH and OD. (a) Extrapolation of experimental data as performed in ref 15. (b) Extrapolation of data from a high-level ab initio calculation of the same state (see text). To mimic the situation occurring in the experimental fit, the last gap has not been considered in the fit. This clearly shows that the curves underestimate the position of the last gap. They also seriously underestimate the resulting dissociation energy. (c) Extrapolation of the same data as in part a but with inclusion of all vibrational levels. The lower order fit clearly shows an inflection point close to the last vibrational gap followed by curvature outward. This behavior is not reproduced in parts a and b and is the primary reason leading to an underestimate of the dissociation energy, whereas the higher order fits do not converge, showing that the underlying Dunham approximation becomes inappropriate in the vicinity of the dissociation limit.

The curves are a plot of these maxima against  $N(N + 1)$ . The parameters  $D_e$  and  $\alpha$  of the Morse potential  $U_0(r)$  have been

iteratively adjusted so that the curves pass exactly through the chosen pairs of points. Given the rather approximate nature of this approach,<sup>80</sup> the values obtained from these curves have to be taken with considerable caution. Nevertheless, although the straight lines of Carlone and Dalby bracket a  $D_0(\text{OH}, \text{B}^2\Sigma^+)$  range of 849–983  $\text{cm}^{-1}$  (or  $916 \pm 67 \text{ cm}^{-1}$ ), the range bracketed by the two limiting curves of dissociation is 906–1016  $\text{cm}^{-1}$  ( $961 \pm 55 \text{ cm}^{-1}$ ) or another  $\sim 50 \text{ cm}^{-1}$  higher. If taken at face value, the estimated  $D_0(\text{OH}, \text{B}^2\Sigma^+) = 961 \pm 55 \text{ cm}^{-1}$  implies  $D_0(\text{OH}, \text{A}^2\Sigma^+) = 19002 \pm 55 \text{ cm}^{-1}$ , or  $\sim 135 \text{ cm}^{-1}$  higher than that from the technically correct Birge–Sponer extrapolation. This value for  $D_0(\text{OH}, \text{B}^2\Sigma^+)$  ultimately implies  $D_0(\text{H–OH}) = 41146 \pm 56 \text{ cm}^{-1}$ , in excellent accord with  $D_0(\text{H–OH}) = 41128 \pm 24 \text{ cm}^{-1}$  suggested above from photoionization experiments. Thus, the reconciliation of the A and B state spectroscopic analysis and the reconciliation of the spectroscopic and photoionization determinations of bond dissociation energies can be both achieved if the technically correct Birge–Sponer underestimates  $D_0(\text{OH}, \text{A}^2\Sigma^+)$  by  $\sim 135 \text{ cm}^{-1}$ .

The last step in our analysis is the incorporation of electronic structure calculations on the  $\text{OH}(\text{A}^2\Sigma^+)$  potential curve. We have carried out multireference single and double excitation (CAS+1+2 with Davidson correction) calculations<sup>81</sup> on the  $\text{OH}(\text{A}^2\Sigma^+)$  potential energy curve with an aug-cc-pV5Z basis set.<sup>50</sup> As will become quite clear in the next section, this level of calculation cannot be expected to produce a dissociation energy accurate to 135  $\text{cm}^{-1}$  and thus cannot “replace” the Birge–Sponer analysis of the spectroscopic data. However, it is expected that this level of theory will reproduce the essential features of the real potential used in the Birge–Sponer analysis. Then the computed dissociation energy can be compared to that derived from the Birge–Sponer analysis on the vibrational eigenstates produced by the computed curve. Indeed, solving the vibrational eigenstates for the calculated potential<sup>82</sup> produces exactly the same number of bound levels<sup>83</sup> (up to  $v = 10$  in OH and  $v = 14$  in OD) as that deduced experimentally by Carlone and Dalby. Figure 5b shows the result of the Birge–Sponer extrapolation using the theoretical levels that are analogous to those observed experimentally. Quite clearly, the extrapolation seriously underestimates the position of the last, experimentally unobserved  $\Delta G(v + 1/2)$  value. The underestimate of the calculated limit is even more severe: the averages of three fits completely analogous to those used by Carlone and Dalby undervalue the calculated limit by 128  $\text{cm}^{-1}$  in OH and 81  $\text{cm}^{-1}$  in OD. If one uses the technically correct integration, the discrepancies are only slightly lower (109  $\text{cm}^{-1}$  for OH and 73  $\text{cm}^{-1}$  for OD). This exercise shows quite persuasively that the Birge–Sponer treatment of the experimental data for  $\text{A}^2\Sigma^+$  of OH and OD leads to a substantial underestimate of the dissociation energy and hence vitiates the most powerful argument (“short” extrapolation) favoring the values derived by Carlone and Dalby. Furthermore, the scale of the underestimation is near that required to resolve the discrepancy with the B state and with the photoionization studies.

An interesting question is whether the experimental knowledge of *all* vibrational levels would have produced a better Birge–Sponer fit. Figure 5c shows such a fit using all calculated  $\Delta G(v + 1/2)$ . The last  $\Delta G(v + 1/2)$  induces a change in curvature of the fitted function close to the dissociation limit. Whereas polynomial fits with  $n = 6$  (and higher) *diverge* both in OH and OD, never producing a  $(v + 1/2)_{\text{intercept}}$  value, fits with  $n = 4$  and 5 behave apparently reasonably and produce similar results close to the calculated limit (13  $\text{cm}^{-1}$  low in OH and 9  $\text{cm}^{-1}$

low in OD, on the average). The corresponding  $v_{\text{max}}$  values are almost 0.5 higher than values obtained by the fit that omits the last vibrational level.<sup>84</sup>

The fact that fits that include all vibrational levels have a tendency to diverge strongly suggests that the polynomial expansion of eq 6 becomes an inadequate representation of  $G(v)$  as the dissociation limit is being approached. This is not surprising at all, because the polynomial expression used in the Birge–Sponer fit is based on the Dunham power series expansion<sup>38</sup> of the diatomic potential about the equilibrium distance  $r_e$ . This gives rise to a reasonable representation close to the bottom of the well, but because the convergence radius for this expansion is  $r_e$ , the power series becomes an inherently inappropriate representation of spectral data when  $r > 2r_e$ .<sup>39</sup>

As opposed to the Dunham polynomial expansion, at large internuclear distances, the potential follows the familiar inverse power form. If only the leading inverse power term is considered, simple expressions for vibrational terms close to the dissociation limit can be derived.<sup>85,86</sup> Such expressions can be extended toward levels that are more bound via empirical functions<sup>87</sup> or (more rigorously) Padé approximants,<sup>87–89</sup> which effectively produce an analytical continuation of Dunham’s expression. For the  $\text{A}^2\Sigma^+$  state, the leading inverse power term is the induced-dipole–induced-dipole  $r^{-6}$  term. There is no experimental measurement of the associated  $C_6$  constant. However, the electronic structure calculations were systematically carried out to  $r = \sim 10 \text{ \AA}$ . An  $r^{-6}$  term with a  $C_6$  value of  $59620 \text{ \AA}^6 \text{ cm}^{-1}$  describes the potential to within 5% from about the turning point of the second to last level of OH ( $\sim 2.5 \text{ \AA}$ ) on out to the asymptote.

Knowledge of the  $r^{-6}$  form and perhaps also of the computed value of the  $C_6$  constant could in principle be incorporated into the analysis of the  $\text{A}^2\Sigma^+$  vibrational levels to produce a more confident estimate of  $D_0$  than that of the usual Birge–Sponer method. Following a suggestion originally given to us by Field,<sup>90</sup> we have attempted to fit both the experimental and computed vibrational levels by using such expressions. The most successful of our numerous attempts involved Padé approximants. For example, the extrapolation of the RKR experimental curve<sup>91</sup> (shown in Figure 6) out to the asymptote could be done with a simple Padé approximant:

$$V_{\text{extrp}}(r) = D - \{(1 + p/r)/(1 + q/r)\}(C_6/r^6), \quad r \geq r_m \quad (8)$$

where  $r_m$  is a match point at which  $p$  and  $q$  of the Padé approximant (in braces) are adjusted to reproduce the RKR potential curve in slope and value. The second term in the above expression expands into an infinite order inverse power series of which the lead term is  $-C_6/r^6$  taken from the ab initio calculations. (This is true only asymptotically: inappropriate  $p$  and  $q$  values can lead to potentials with barriers or singularities in physically meaningful regions of  $r$ .) In  $V_{\text{extrp}}(r)$ , the dissociation energy  $D$  is an adjustable parameter selected so as to optimally fit in a least squares sense a local region on the RKR curve about the match point  $r_m$ . If there is any information in the RKR curve that constrains the dissociation energy, in eq 8, it is reflected in the adjustable value of  $D$  only through the local region about  $r_m$ . The final potential curve is then the RKR curve for  $r \leq r_m$  and  $V_{\text{extrp}}$  for  $r \geq r_m$ . Correspondingly, the Birge–Sponer estimate of  $D_0$  is replaced by the adjusted value of the parameter  $D$  minus the ZPE.

A major difficulty with extrapolation schemes, whether they be for potential curves or  $G(v)$ , is that there is no rigorous way to select a local region from which to adjust the dissociation energy. The most successful approach discovered involved a

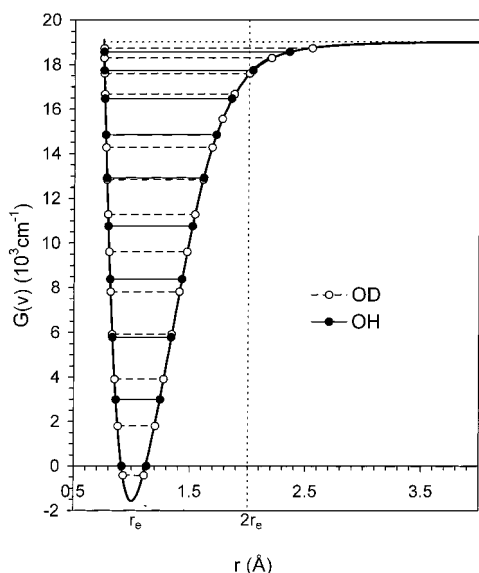


**Figure 6.** RKR curve for the  $A^2\Sigma^+$  state of OH (full circles) and OD (open circles). The last two levels in each of the two isotopomers are outside the  $2r_e$  region (which is the domain of validity of the Dunham approximation) yet barely start encroaching on the long-range region of the potential and hence do not carry a strong information content on the long-range behavior of the potential.

sequence of local regions of  $2\Delta r$  in width centered about the sequence of  $r_m$  values of the form  $\{r_{m,i} = r_{\text{htp}} - i\Delta r \mid i = 1, n\}$ , where  $r_{\text{htp}}$  is the RKR turning point for the highest observed level. The  $i$ th local region can be processed to obtain an optimal  $D_i$  value. The resulting  $D_i$  values as a function of  $r_{m,i}$  are observed to decay largely exponentially to an asymptotic value at large  $r$  for OH and OD for both the experimental RKR curve and the ab initio potential curve. This asymptotic  $D_\infty$  can be interpreted as the value eq 8 would have produced if the data would have allowed the  $r_m$  sequence to be extended beyond  $r_{\text{htp}}$ . The final value of  $D_\infty$  does depend on the choice of  $\Delta r$ . If  $\Delta r$  is too small, any value of  $D_i$  fits the data well giving rise to unphysical or poorly fit extrapolations to  $D_\infty$ . The same can also be true if  $\Delta r$  is too large because some values of  $D_i$  are determined by too much of the interior portion of the potential energy curve where there is little dissociation energy sensitivity. However, for a range of  $\Delta r$  in the vicinity of  $\sim 0.1$  Å, well behaved extrapolations to physically meaningful values of  $D_\infty$  can be achieved. Depending on the order of the Dunham expansions used in the RKR analysis,<sup>91</sup> the final values of  $D_0$  determined from  $D_\infty$  are  $18956 \pm 14$   $\text{cm}^{-1}$  for  $D_0(\text{OH}, A^2\Sigma^+)$  and  $19365 \pm 15$   $\text{cm}^{-1}$  for  $D_0(\text{OD}, A^2\Sigma^+)$ . When the same procedure is applied to the ab initio curve using the analogous highest observed level to set  $r_{\text{htp}}$ , the resulting  $D_\infty$  values for OH and OD are 20146 and 20120  $\text{cm}^{-1}$ , respectively, where the correct computed  $D_e$  is 20121  $\text{cm}^{-1}$ , i.e., a 25  $\text{cm}^{-1}$  error or less. The value of  $D_\infty$  does depend on the value of  $C_6$  used, but only to a minor degree. Variation of the  $C_6$  value by  $\pm 10\%$  produced alterations in  $D_0$  that fall within the  $\sim 15$   $\text{cm}^{-1}$  error bars produced by different RKR curves.

Although suggestive, this analysis is not definitive because it is not robust. The implications of wide variations in the selected value for  $\Delta r$  have already been mentioned. In addition, simple variations of eq 8 do not produce sensible results. For example, in eq 8,  $p$  could be set to zero and  $d$  and  $q$  directly selected so as to match slope and value at each  $r_{m,i}$ . The resulting sequence of  $D_i$  can be extrapolated to  $D_\infty$ , but the extrapolated value is typically below the highest observed level. There is also a “chatter” in the values of  $D_i$  as  $r_{m,i}$  approaches  $r_{\text{htp}}$  that

fitting over a local region of  $2\Delta r$  as required by eq 8 apparently averages out. Alternatively, one could add a  $P'/r^2$  term to the numerator of the Padé approximant in eq 8 resulting in two parameters (say  $D$  and  $P'$ ) to adjust in optimizing agreement over the local region between the extrapolated form and the RKR curve. This leads to erratic values of  $D_i$  that do not allow a reliable extrapolation to  $D_\infty$ . Despite the lack of robustness, the procedure discussed above, which incorporates new information in the form of an ab initio  $C_6$  value, implies that the technically correct Birge–Sponer value for  $D_0(\text{OH}, A^2\Sigma^+)$  of 18866.7  $\text{cm}^{-1}$  is too low by  $89 \pm 14$   $\text{cm}^{-1}$ . The new estimates for  $D_0(A^2\Sigma^+)$  imply  $D_0(\text{OH}) = 35529 \pm 14$   $\text{cm}^{-1}$ , a value lower than the photoionization estimate of  $35593 \pm 24$   $\text{cm}^{-1}$  by only by 64  $\text{cm}^{-1}$ .

Whereas the above discussion has focused on extrapolating the RKR potential curves, a similar discussion can be carried out for directly extrapolating the  $G(v)$  function because the form of that function for a  $-C_6/r^6$  attractive potential is known.<sup>85,86</sup> Extrapolation of  $G(v)$  from the observed levels to this asymptotic form can also be accomplished by Padé approximants<sup>92</sup> and the same questions of appropriate fitting regions and of robustness with respect to the Padé form limit the confidence one can have in the results. However, such analysis does suggest an inflection point and a consequent drastic change in the curvature of  $G(v)$  beyond the last experimental point. The existence of an inflection point guarantees that any Birge–Sponer type of extrapolation that maintains the general direction of curvature implied by the points before the inflection will systematically underestimate  $v_{\text{max}}$  and hence  $D_0$ .

The difficulty of extrapolating either the RKR potential or  $G(v)$  to the asymptote probably arises from the fact that the last few vibrational states of the  $A^2\Sigma^+$  state are just outside the validity domain of the Dunham expansion region, yet barely start encroaching on the long-range region of the potential. Consequently, they do not protrude far enough to carry a strong information content on the long-range behavior of the potential, leading to difficulties in extracting that information with confidence. This explanation is corroborated by the experience of applying extrapolation procedures to the ab initio potential, which is shallower than the experimental potential by several hundred wavenumbers and consequently has turning points for the highest vibrational levels that are at larger  $r$  than those obtained from the RKR analysis. For example, the second to last OD level has an ab initio turning point of 2.84 Å, whereas the corresponding value on the experimental RKR potential is 2.55 Å. In general, extrapolation of the ab initio potential is less sensitive to the definition of a fitting region and more tolerant of variation in the form of the extrapolating function than extrapolation on experimental data.

From all of the above analysis on both the  $A^2\Sigma^+$  and  $B^2\Sigma^+$  states of OH and OD, we can conclude that the original analysis of Carlone and Dalby underestimates the  $D_0(\text{OH})$  by a thermodynamically significant amount. In the case of the  $A^2\Sigma^+$  state, a Birge–Sponer extrapolation over only one missing level still introduces a significant underestimation of  $D_0(\text{OH}, A^2\Sigma^+)$  because the missing level has a changed character that reflects the influence of long-range forces. In the case of the  $B^2\Sigma^+$  state, an overly approximate treatment of the centrifugal barrier leads to an underestimation of  $D_0(\text{OH}, B^2\Sigma^+)$ . In both cases, more sophisticated but still approximate analysis and, for the  $A^2\Sigma^+$  state, additional ab initio information suggest that  $D_0(\text{OH})$  is underestimated by  $\sim 110$   $\text{cm}^{-1}$  (for  $A^2\Sigma^+$ ) and  $\sim 155$   $\text{cm}^{-1}$  (for  $B^2\Sigma^+$ ). The photoionization results of the previous section suggest an underestimation by  $172 \pm 25$   $\text{cm}^{-1}$ . Thus, this review



of the Carlone and Dalby results can largely but not perfectly reconcile the spectroscopic and photoionization data. It is likely that only new measurements on either the  $A^2\Sigma^+$  and  $B^2\Sigma^+$  states can tighten the estimates of  $D_0(\text{OH})$  from the spectroscopic data.

#### 4. Theoretical Studies

In this section, we report ab initio calculations that are designed to directly determine the thermodynamic quantities of interest in this paper to an accuracy of about  $50\text{ cm}^{-1}$  ( $\sim 0.10$  to  $\sim 0.20$  kcal/mol). This will involve the determination of atomization energies, ionization potentials, and dissociation energies. First we describe the electronic structure methods used, and then we report and discuss the results.

**4.1. Methods.** All ab initio calculations presented in this section were carried out by using MOLPRO,<sup>93</sup> Gaussian 98,<sup>94</sup> and ACESII<sup>95</sup> on an SGI Origin 2000 or an SGI PowerChallenge computer.

The computational procedure for obtaining atomization energies starts with CCSD(T) electronic energies including only the valence electrons in the correlation calculation extrapolated to the complete basis set (CBS) limit, a step which is facilitated by the uniform convergence properties of the correlation consistent basis sets (cc-pVnZ) from Dunning and co-workers.<sup>50</sup> For the present study, we used the diffuse function augmented (aug-cc-pVnZ) basis sets for  $n = \text{T, Q, 5}$  and  $6$ . In addition, we were able to carry out calculations using an “unofficial” septuple- $\zeta$  basis set that was designed to mimic the correlation consistent approach. In all cases only the spherical components (5-*d*, 7-*f*, 9-*g*, 11-*h*, and 13-*i*) of the Cartesian basis functions were used. Because of software limitations, we were unable to include *k* functions ( $l = 7$ , where  $l$  is the angular momentum quantum number) in the aug-cc-pV7Z basis set. The small energy contribution from the missing functions was estimated by extrapolating the contributions of the *h*- ( $l = 5$ ) and *i*-type functions ( $l = 6$ ). A check on the accuracy of this extrapolation for the oxygen atom at the singles and doubles configuration interaction level of theory showed it to be good to at least  $10^{-5}$  Hartrees.<sup>96</sup>

Three coupled cluster methods have been proposed for treating open shell systems. The first is a completely unrestricted method, built atop unrestricted Hartree–Fock (UHF) orbitals and designated UCCSD(T). The other two methods start with restricted open shell Hartree–Fock (ROHF) orbitals. One is a completely restricted method, which we label as RCCSD(T).<sup>97</sup> The other relaxes the spin constraint in the coupled cluster calculation and is designated R/UCCSD(T).<sup>98</sup> At present, little is known about which open shell coupled cluster method produces the best agreement with the exact full configuration interaction (FCI) results. In prior FCI work on AH and AB diatomics,<sup>99–101</sup> cc-pVDZ basis set results were often found to be unreliable in predicting the true effect of higher order correlation recovery beyond the CCSD(T) method. Thus, if FCI calculations are to be useful in calibrating coupled cluster results, it appears that basis sets of at least triple- $\zeta$  quality will be necessary, severely restricting the number of systems that can be examined. Consequently, in previous work, we have tended to use the spread in atomization energies resulting from the three open shell coupled cluster methods as an indicator of the uncertainty in our findings. However, for this study, we were able to carry out a FCI/cc-pVTZ calculation on OH ( $^2\Pi$ ) and a FCI on H<sub>2</sub>O ( $^1A_1$ ) with a combination of the cc-pVTZ basis set on oxygen and the cc-pVDZ basis set on hydrogen. The latter calculation involved  $1.7 \times 10^9$  determinants and was performed with the Knowles sparsity-driven, determinant-based FCI pro-

gram.<sup>102</sup> Program thresholds were chosen to ensure accuracy in the total energy to at least  $10^{-5}$  Hartrees.

In the case of OH, where an open shell molecule dissociates into two open shell atoms, the spread in dissociation energies across the three CCSD(T) methods was a mere 0.07 kcal/mol. All three methods underestimated the FCI result, with errors ranging from 0.06 to 0.13 kcal/mol. The R/UCCSD(T) and RCCSD(T) methods produced essentially identical results and were in best agreement with FCI. For H<sub>2</sub>O, the spread in atomization energies was a somewhat larger 0.17 kcal/mol, with the R/UCCSD(T) method coming closest to reproducing the FCI result,  $\Sigma D_e = 216.29$  (FCI) vs 216.27 (R/UCCSD(T)) kcal/mol, a difference of  $-0.02$  kcal/mol. Errors for the RCCSD(T) and UCCSD(T) methods were only slightly larger, at  $+0.06$  and  $-0.12$  kcal/mol, respectively. On the basis of these results, we have adopted the R/UCCSD(T) results for open shell systems, although the very limited amount of data precludes making generalizations for other systems or for larger basis sets.

In previous studies,<sup>100,101,103</sup> we have sometimes estimated the difference between FCI and CCSD(T) with the CCSDT method in which triple excitations are treated on the same footing as the singles and doubles, i.e., iteratively via the coupled cluster equations.<sup>104</sup> For a collection of 25 known FCI energies, CCSDT shows a slightly smaller mean absolute deviation than does CCSD(T). However, the level of agreement between CCSDT and FCI was found to vary significantly among the molecules in the test set. In the case of H<sub>2</sub>O, CCSDT actually predicts a reduction in the atomization energy, relative to CCSD(T), whereas FCI increases the atomization energy.

Three different formulas were used to extrapolate the correlation energy to the frozen core CBS limit. The first is a three-parameter function in  $1/l_{\text{max}}$ , where  $l_{\text{max}}$  is the highest angular momentum in the oxygen basis set:<sup>105</sup>

$$E(l_{\text{max}}) = E_{\text{CBS}} + B/l_{\text{max}}^3 + C/l_{\text{max}}^4 \quad (9a)$$

where  $l_{\text{max}} = 2$  (DZ), 3 (TZ), etc. In addition, we used two two-parameter formulas<sup>106,107</sup>

$$E(l_{\text{max}}) = E_{\text{CBS}} + B/(l_{\text{max}} + 1/2)^4 \quad (9b)$$

and

$$E(l_{\text{max}}) = E_{\text{CBS}} + B/l_{\text{max}}^3 \quad (9c)$$

In previous work, we have used a mixed exponential-Gaussian form<sup>108</sup>

$$E(l_{\text{max}}) = E_{\text{CBS}} + Be^{-(l_{\text{max}}^{-1})} + Ce^{-(l_{\text{max}}^{-1})^2} \quad (9d)$$

which on average has been found to produce slightly better agreement with experiment when basis sets up to quadruple- $\zeta$  were available. However, the  $1/l_{\text{max}}$  formulas, which are based on the asymptotic  $1/Z$  perturbation theory convergence properties of two-electron systems,<sup>106</sup> as well as principal expansion arguments,<sup>107</sup> are thought to perform better for the very large basis sets employed in the present work. We adopt the average of the three extrapolations as our best estimate of the frozen core CBS limit. The assignment of meaningful error bars to the present theoretical results is hindered by the general lack of formal, a priori error bars for all electronic structure calculations. After careful consideration, we have adopted three times the spread among the estimated CBS limits as a crude measure of our uncertainty.<sup>109</sup> This choice reflects the uncertainty in the CBS energies, as well as errors arising from a number of smaller

corrections, to be discussed, and the assumption that these smaller corrections are additive. In each case, the CBS extrapolations based on eqs 9a–c involved only the R/UCCSD(T) correlation energies. The resulting CBS limits were then obtained by combining the extrapolated correlation energies with the SCF/aug-cc-pV7Z total energies.

The geometries were optimized at the frozen core CCSD(T) level of theory. The molecular zero-point energies were taken from the experiment and include anharmonic corrections.<sup>40,52,110</sup> Additional corrections to the CCSD(T)(FC) atomization energies are needed when trying to achieve accuracies on the order of a few tenths of a kcal/mol. Core/valence corrections ( $\Delta E_{CV}$ ) to the dissociation energy were obtained from fully correlated CCSD(T) calculations with the cc-pCV5Z basis sets<sup>50</sup> at the CCSD(T)/aug-cc-pVTZ geometries.

The effects of relativity must also be considered. Most electronic structure computer codes do not correctly describe the lowest energy spin multiplet of an atomic state, such as the  $^3P$  state of oxygen. Instead, the computed energy corresponds to a weighted average of the available multiplets. To correct for this effect, we apply an atomic spin–orbit correction of  $-78 \text{ cm}^{-1}$  for O on the basis of the excitation energies of Moore.<sup>66</sup> For OH, a molecular spin–orbit correction of  $-38.18 \text{ cm}^{-1}$  is also available from experiment.<sup>36,40,111</sup>

Molecular scalar relativistic corrections ( $\Delta E_{SR}$ ) which account for changes in the relativistic contributions to the total energies of the molecule and the constituent atoms were included at the CCSD(T) level of theory using an uncontracted cc-pVQZ basis set in the frozen core approximation.  $\Delta E_{SR}$  is taken as the sum of the mass-velocity and one-electron Darwin (MVD) terms in the Breit–Pauli Hamiltonian.<sup>112</sup>  $\Delta E_{SR}$  is very insensitive to the level of theory. The present CCSD(T) values are within  $10^{-4}$  Hartrees of values obtained at the singles and doubles CI level, a method we have applied previously, and differences in differential scalar relativistic corrections for atomization energies are even smaller.

Finally, corrections that are due to the Born–Oppenheimer approximation have also been included by calculating the diagonal correction (BODC). These calculations used the formulas as implemented in MOLPRO by Schwenke<sup>113</sup> at the complete active space self-consistent field level (CASSCF) with the aug-cc-pVTZ basis set. The active space used in these calculations, which were carried out in  $C_s$  symmetry, involved 7  $a'$  and 2  $a''$  orbitals with eight electrons active (the first  $a'$  orbital constrained to be doubly occupied). Following the suggestion of Handy and Lee,<sup>114</sup> atomic masses were used throughout,<sup>115</sup> and these values, including conversion factors, were obtained from the NIST website, <http://www.physics.nist.gov/PhysRefData/contents.html>.

**4.2. Results and Discussion.** Figure 7 shows the regularity of the frozen core correlation energy of  $\text{H}_2\text{O}$  and OH as a function of the basis set size, along with the CBS limit estimates obtained from eq 9c. As one can see, even basis sets as large as aug-cc-pV7Z are still relatively far from the limit, reflecting the well-known slow convergence of the one-particle expansion. Table 2 lists the R/UCCSD(T)/aug-cc-pVnZ,  $n = Q, 5, 6,$  and 7, frozen core total electronic energies and CBS extrapolations using eqs 9a–c. Table 3 shows the corresponding convergence behavior of IE(O), IE(OH),  $\Delta E_{\text{atomiz}}(\text{H}_2\text{O})$ ,  $D_e(\text{H–OH})$ , and  $D_e(\text{OH})$ . For IE(O) and IE(OH), the extrapolations are seen to be relatively insensitive to the size of the underlying basis sets, because the use of basis sets up to aug-cc-pV7Z results in essentially no change in the IEs as compared to using basis sets only up to the aug-cc-pV6Z ones. For  $\Delta E_{\text{atomiz}}(\text{H}_2\text{O})$ , all

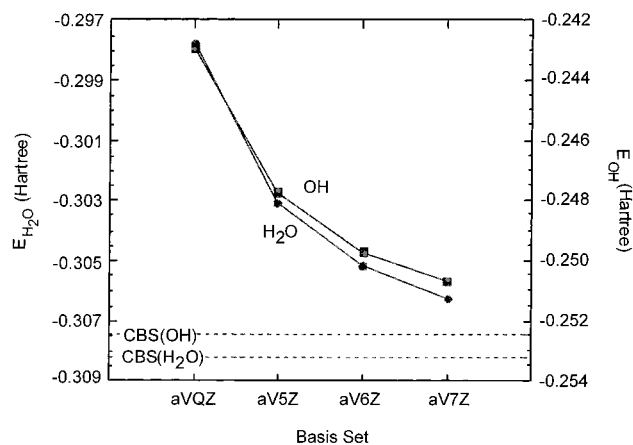


**Figure 7.** Frozen core CCSD(T) correlation energy of  $\text{H}_2\text{O}$  and OH as a function of the basis set size. The estimated CBS limits were obtained from the two point  $E(n) = E_{\text{CBS}} + B/l_{\text{max}}^3$  formula using the aug-cc-pV6Z and aug-cc-pV7Z basis sets.

three formulas behave similarly, increasing the computed value by  $\sim 0.2 \text{ kcal/mol}$  when the aug-cc-pV7Z basis set is used as the largest basis set.  $D_e(\text{OH})$  and  $D_e(\text{H–OH})$  behave very similarly to the atomization energy of water, although the changes are about a factor of 2 smaller ( $\sim 0.1 \text{ kcal/mol}$ ).

Table 4 lists the corrections for core–valence and scalar relativistic effects, and the amount of higher order correlation recovery. Together with the experimental ZPEs, spin–orbit effects, and diagonal Born–Oppenheimer corrections, the estimated CBS limits lead to the final computed thermochemical quantities. The “error bars” attached to these quantities are a reflection of three times the spread of estimated valence correlation energies using the three CBS extrapolation formulas (9a–c). This conservative estimate of the extrapolation error is designed to also include systematic errors in the additional small correction factors incorporated into the final computed quantities. The magnitudes of the small correction factors show how difficult it is to calculate dissociation energies to a few tenths of a kcal/mol. The core valence correction  $\Delta E_{CV}$  ranges from 0.14 to 0.36 kcal/mol, always increasing the energy, and the scalar relativistic correction  $\Delta E_{SR}$  is always negative for these energies ranging from  $-0.12$  to  $-0.27$ . The smallest magnitude of these corrections is found for  $D_0(\text{OH})$ . The full-CI correction  $\Delta E_{\text{FCI}}$  is less than 0.1 kcal/mol and is largest for OH where it increases the dissociation energy by 0.08 kcal/mol. The smallest  $\Delta E_{\text{FCI}}$  correction is for  $D_0(\text{H–OH})$  where it is only  $-0.02 \text{ kcal/mol}$ . The diagonal Born–Oppenheimer correction  $\Delta E_{\text{BODC}}$  is very small for OH, only  $-0.01 \text{ kcal/mol}$ , but is significantly larger for  $D_0(\text{H–OH})$ , 0.11 kcal/mol, and for  $\Delta H_{\text{atomiz},0}^{\text{p}}(\text{H}_2\text{O})$ , it is 0.10 kcal/mol. Clearly, target accuracies of a tenth of a kcal/mol will require consideration of this term in the calculation of the atomization energy. At this point, it should also be noted that nonadiabatic corrections to the zero-point energy of  $\text{H}_2\text{O}$  are calculated using the method of ref 113 to be only  $0.23 \text{ cm}^{-1}$ , which will have no effect on the present results.

The computed values for  $\Delta H_{\text{atomiz},0}^{\text{p}}(\text{H}_2\text{O})$ , IE(OH), and IE(O) serve as a benchmark for our theoretical approach. When results only up to the 6- $\zeta$  level are included, the theoretical atomization energy of water is smaller than the experimental value by 0.05 kcal/mol, IE(OH) by 0.02 kcal/mol, and IE(O) by 0.10 kcal/mol. The errors with respect to experiment in Table 4 are comparable to the theoretical error bars, lending credence to their use as crude measures of the inherent uncertainty in the calculations.

**TABLE 2: R/UCCSD(T) Frozen Core and Estimated Complete Basis Set (CBS) Frozen Core Electronic Energies for O, O<sup>+</sup>, OH, OH<sup>+</sup>, and H<sub>2</sub>O<sup>a</sup>**

basis	O ( <sup>3</sup> P)	O <sup>+</sup> ( <sup>4</sup> S)	OH (X <sup>2</sup> Π)	OH <sup>+</sup> (X <sup>3</sup> Σ <sup>-</sup> )	H <sub>2</sub> O ( <sup>1</sup> A <sub>1</sub> )
aug-cc-pVQZ	-74.995132	-74.498352	-75.664450	-75.187268	-76.363587
aug-cc-pV5Z	-75.000610	-74.502402	-75.670573	-75.192346	-76.370298
aug-cc-pV6Z	-75.002425	-74.503580	-75.672631	-75.193932	-76.372558
CBS( <i>l</i> <sub>max</sub> <sup>3,4</sup> ) <sub>Q56</sub> <sup>b</sup>	-75.004456	-74.504735	-75.674895	-75.195512	-76.374940
CBS( <i>l</i> <sub>max</sub> <sup>4</sup> ) <sub>56</sub> <sup>c</sup>	-75.004206	-74.504697	-75.674672	-75.195437	-76.374753
CBS( <i>l</i> <sub>max</sub> <sup>3</sup> ) <sub>56</sub> <sup>d</sup>	-75.004744	-74.505034	-75.675291	-75.195894	-76.375419
aug-cc-pV7Z <sup>e</sup>	-75.003283	-74.504111	-75.673654	-75.194709	-76.373714
CBS( <i>l</i> <sub>max</sub> <sup>3,4</sup> ) <sub>567</sub> <sup>b</sup>	-75.004622	-74.504919	-75.675337	-75.196031	-76.375702
CBS( <i>l</i> <sub>max</sub> <sup>4</sup> ) <sub>67</sub> <sup>c</sup>	-75.004368	-74.504778	-75.674958	-75.195703	-76.375186
CBS( <i>l</i> <sub>max</sub> <sup>3</sup> ) <sub>67</sub> <sup>d</sup>	-75.004708	-74.504987	-75.675367	-75.196015	-76.375648

<sup>a</sup> Energies are in Hartrees. Optimal CCSD(T) geometries were used, with the exception of the aug-cc-pV7Z results, which were performed at the optimal aug-cc-pV6Z geometry. OH:  $r_{\text{OH}} = 0.9707$  (aug-cc-pVQZ), 0.9702 (aug-cc-pV5Z), and 0.9701 Å (aug-cc-pV6Z). OH<sup>+</sup>:  $r_{\text{OH}} = 1.0283$  (aug-cc-pVQZ), 1.0280 (aug-cc-pV5Z), and 1.0279 Å (aug-cc-pV6Z). H<sub>2</sub>O:  $r_{\text{OH}} = 0.9594$  (aug-cc-pVQZ), 0.9584 (aug-cc-pV5Z), and 0.9577 Å (aug-cc-pV6Z).  $\angle\text{HOH} = 104.35^\circ$  (aug-cc-pVQZ), 104.43° (aug-cc-pV5Z), and 104.40° (aug-cc-pV6Z). Symmetry equivalencing of the OH ( $\pi_x$ ,  $\pi_y$ ) and oxygen ( $p_x$ ,  $p_y$ ,  $p_z$ ) atomic orbitals was not imposed. The Hartree-Fock energies for the H atom are -0.4999483 (aug-cc-pVQZ), -0.4999948 (aug-cc-pV5Z), -0.4999993 (aug-cc-pV6Z), and -0.4999997 (aug-cc-pV7Z). The CBS limit for H-atom is taken as exactly -0.500E<sub>h</sub>. The HF/aug-cc-pV7Z total energies that were used in the CBS limit determinations were -74.812392 (O), -74.372602 (O<sup>+</sup>), -75.422943 (OH), -75.002149 (OH<sup>+</sup>), and -76.067437 (H<sub>2</sub>O). <sup>b</sup> R/UCCSD(T)(FC) CBS extrapolation based on the  $1/l_{\text{max}}^3 + 1/l_{\text{max}}^4$  formula. <sup>c</sup> R/UCCSD(T)(FC) CBS extrapolation based on the  $1/(l_{\text{max}} + 1/2)^4$  formula. <sup>d</sup> R/UCCSD(T)(FC) CBS extrapolation based on the  $1/l_{\text{max}}^3$  formula. <sup>e</sup> Because of a limitation in the MOLPRO integral package, we were unable to include  $k$  functions in the oxygen basis set. Their small energy contribution ( $\sim -0.00030$  Hartrees) was estimated by performing an exponential extrapolation using the contributions of the  $h$  ( $l = 5$ ) and  $i$  ( $l = 6$ ) functions. Tests of this approach at the CISD level of theory using a code capable of handling  $k$  functions suggests that the extrapolation should be accurate to  $10^{-5}$  Hartree or better.

**TABLE 3: Convergence Behavior for  $\Delta E_{\text{Atomiz,e}}(\text{H}_2\text{O})$ , IE(O), IE(OH),  $D_e(\text{H-OH})$ , and  $D_e(\text{OH})^a$** 

basis	IE(O)	IE(OH)	$\Delta E_{\text{Atomiz,e}}(\text{H}_2\text{O})$	$D_e(\text{H-OH})$	$D_e(\text{OH})$
aug-cc-pVQZ	311.734	299.436	231.274	124.993	106.281
aug-cc-pV5Z	312.630	300.092	231.989	125.332	106.657
aug-cc-pV6Z	313.030	300.388	232.263	125.457	106.807
CBS( <i>l</i> <sub>max</sub> <sup>3,4</sup> ) <sub>Q56</sub> <sup>b</sup>	313.58	300.82	232.48	125.53	106.95
CBS( <i>l</i> <sub>max</sub> <sup>4</sup> ) <sub>56</sub> <sup>c</sup>	313.45	300.72	232.52	125.55	106.97
CBS( <i>l</i> <sub>max</sub> <sup>3</sup> ) <sub>56</sub> <sup>d</sup>	313.57	300.83	232.60	125.58	107.02
CBS <sub>Q56aver</sub> <sup>e</sup>	313.53 ± 0.20	300.79 ± 0.18	232.54 ± 0.21	125.55 ± 0.09	106.98 ± 0.12
aug-cc-pV7Z <sup>e</sup>	313.235	300.543	232.449	125.540	106.909
CBS( <i>l</i> <sub>max</sub> <sup>3,4</sup> ) <sub>567</sub> <sup>b</sup>	313.57	300.77	232.86	125.73	107.13
CBS( <i>l</i> <sub>max</sub> <sup>4</sup> ) <sub>67</sub> <sup>c</sup>	313.50	300.74	232.69	125.64	107.05
CBS( <i>l</i> <sub>max</sub> <sup>3</sup> ) <sub>67</sub> <sup>d</sup>	313.58	300.80	232.77	125.68	107.09
CBS <sub>5/67aver</sub> <sup>f</sup>	313.55 ± 0.15	300.77 ± 0.09	232.77 ± 0.24	125.68 ± 0.15	107.09 ± 0.12
CBS <sub>5/67aver</sub> - CBS <sub>Q56aver</sub>	0.02	-0.02	0.23	0.13	0.11

<sup>a</sup> Values are in kcal/mol, based on R/UCCSD(T) frozen core and estimated complete basis set (CBS) electronic energies for O, O<sup>+</sup>, OH, OH<sup>+</sup>, and H<sub>2</sub>O given in Table 2. <sup>b</sup> Based on R/UCCSD(T)(FC) CBS extrapolation using the  $1/l_{\text{max}}^3 + 1/l_{\text{max}}^4$  formula. <sup>c</sup> Based on R/UCCSD(T)(FC) CBS extrapolations using the  $1/(l_{\text{max}} + 1/2)^4$  formula. <sup>d</sup> Based on R/UCCSD(T)(FC) CBS extrapolations using the  $1/l_{\text{max}}^3$  formula. <sup>e</sup> Average of CBS(*l*<sub>max</sub><sup>3,4</sup>)<sub>Q56</sub>, CBS(*l*<sub>max</sub><sup>4</sup>)<sub>56</sub>, and CBS(*l*<sub>max</sub><sup>3</sup>)<sub>56</sub> extrapolations. The uncertainty reflects the spread in the extrapolations. <sup>f</sup> Average of CBS(*l*<sub>max</sub><sup>3,4</sup>)<sub>567</sub>, CBS(*l*<sub>max</sub><sup>4</sup>)<sub>67</sub>, and CBS(*l*<sub>max</sub><sup>3</sup>)<sub>67</sub> extrapolations. The uncertainty reflects the spread in the extrapolations.

The inclusion of the 7- $\zeta$  results in the CBS extrapolation only slightly changes the differences between theory and experiment for IE(O) and IE(OH) but increases that of  $\Delta H_{\text{atomiz0}}^\circ(\text{H}_2\text{O})$  somewhat. The theoretical values now differ from the experimental values by -0.18 kcal/mol for  $\Delta H_{\text{atomiz0}}^\circ(\text{H}_2\text{O})$ , 0.03 kcal/mol for IE(OH) and 0.08 kcal/mol for IE(O).

At this stage in the development of standard electronic structure methods, it is very difficult to judge if the remaining small errors with respect to the experiments come primarily from the extrapolation to the CBS limit or the various smaller corrections. To illustrate the sensitivity of just the CBS component to the five thermochemical properties in Table 4, new extrapolations were performed with the same three formulas (9a-c), but rather than using only the two (or three) largest basis set results, all four results were used in a least squares procedure. By so doing, the deviation with respect to experiment is significantly improved for  $\Delta H_{\text{atomiz0}}^\circ(\text{H}_2\text{O})$ , going from -0.18 to -0.08 kcal/mol. There is a similar improvement in  $D_0(\text{H-OH})$ , whereas IE(O) and  $D_0(\text{OH})$  very slightly worsen, and IE(OH) remains unchanged. The results of the least-squares fitting approach also exhibit improved internal consistency characteristics, e.g., the difference between the CBS<sub>Q56aver</sub> and

CBS<sub>5/67aver</sub> values in Table 3 are now always less than the raw 6- $\zeta$ /7- $\zeta$  difference. This notwithstanding, we have elected to use the CBS energies obtained by extrapolating only the largest basis set values in the belief that they come closer to satisfying the conditions under which the  $1/l_{\text{max}}$  formulas should work best.

Additional insight into the accuracy of our CBS estimates can be gained from very recent calculations using "explicitly correlated R12" techniques which appeared in print while this manuscript was in preparation. Noga et al.<sup>116</sup> report a CCSD(T)-R12 frozen core H<sub>2</sub>O atomization energy of 232.54 kcal/mol (vs 232.77 ± 0.24 for the present work) using a large, uncontracted (spdfgh/spdfg) basis set, where the part before the slash represents oxygen and the part after the slash represents hydrogen. The geometry used in the R12 calculations is very slightly different than the one we have used, causing an expected difference of less than 0.01 kcal/mol in the atomization energy. Because of the independent manner in which the R12 technique estimates the CBS limit, with an avoidance of the need to adopt one or more extrapolation formulas, the similarity of the R12 and current results is encouraging.

As seen from the last column in Table 4, the theoretical value for  $D_0(\text{OH})$  is nearly identical to the experimental value



**TABLE 4: Electronic Energy Contributions to the Calculation of Thermochemical Properties<sup>a</sup>**

component	IE(O)	IE(OH)	$\Delta H_{\text{atomiz0}}^{\circ}(\text{H}_2\text{O})$	$D_0(\text{H}-\text{OH})$	$D_0(\text{OH})$
CBS <sub>5/67aver</sub> <sup>b</sup>	313.55 ± 0.12	300.77 ± 0.09	232.77 ± 0.24	125.68 ± 0.15	107.09 ± 0.12
$\Delta E_{\text{cv}}^{\text{c}}$	0.334	0.270	0.358	0.220	0.138
$\Delta E_{\text{SR}}^{\text{d}}$	-0.208	-0.163	-0.270	-0.151	-0.119
$\Delta E_{\text{FCI}}^{\text{e}}$	0.06	0.05	0.06	-0.02	0.08
$\Delta E_{\text{ZPE}}^{\text{f}}$	—	-0.889	-13.260	-7.969	-5.291
$\Delta E_{\text{SO}}^{\text{g}}$	0.223	0.109	-0.223	-0.109	-0.114
$\Delta E_{\text{BODC}}^{\text{h}}$	—	—	0.10	0.11	-0.01
total	313.96 ± 0.15	300.15 ± 0.09	219.54 ± 0.24	117.76 ± 0.15	101.77 ± 0.12
expt	314.040 ± 0.001 <sup>i</sup>	300.179 ± 0.006 <sup>j</sup>	219.356 ± 0.024 <sup>k</sup>	117.591 ± 0.069 <sup>l</sup>	101.765 ± 0.073 <sup>l</sup>
[expt - calcd]	[0.08]	[0.03]	[-0.18]	[-0.17] <sup>l</sup>	[0.01] <sup>l</sup>
				118.085 ± 0.049 <sup>m</sup>	101.271 ± 0.043 <sup>m</sup>
				[0.33] <sup>m</sup>	[-0.50] <sup>m</sup>
				117.913 ± 0.286 <sup>n</sup>	101.442 ± 0.286 <sup>n</sup>
				[0.15] <sup>n</sup>	[-0.33] <sup>n</sup>
				117.657 ± 0.014 <sup>o</sup>	101.699 ± 0.027 <sup>o</sup>
				[-0.10] <sup>o</sup>	[-0.07] <sup>o</sup>

<sup>a</sup> Values are in kcal/mol. <sup>b</sup> Average of CBS( $I_{\text{max}}^{3,4}$ )<sub>567</sub>, CBS( $I_{\text{max}}^4$ )<sub>67</sub>, and CBS( $I_{\text{max}}^3$ )<sub>67</sub> extrapolation, shown in Table 3. The uncertainty reflects the spread in the extrapolations. <sup>c</sup> Core/valence corrections obtained from R/UCCSD(T)/cc-pCV5Z calculations. <sup>d</sup> Scalar relativistic corrections obtained from R/UCCSD(T)(FC)/unc-cc-pVQZ calculations. <sup>e</sup> A correction to the atomization energy for higher order excitations based on FCI/cc-pVTZ(OH, OH<sup>+</sup>) and FCI/cc-pVTZ/VDZ (H<sub>2</sub>O) calculations. <sup>f</sup> ZPE(H<sub>2</sub>O, X<sup>1</sup>A<sub>1</sub>) = 4637.97 cm<sup>-1</sup> from ref 52 (cf. to 4631.25 cm<sup>-1</sup> from ref 36). ZPE(OH, X<sup>2</sup>Π) = 1850.69 cm<sup>-1</sup> and ZPE(OH<sup>+</sup>, X<sup>3</sup>Σ<sup>-</sup>) = 1539.72 cm<sup>-1</sup> (including Y<sub>00</sub> terms), based on data from ref 40. ZPE(OH<sup>+</sup>, X<sup>3</sup>Σ<sup>-</sup>) includes the F<sub>1</sub>(0) term of -1.46 cm<sup>-1</sup>. <sup>g</sup> Weighted average of <sup>3</sup>P term in O is 78.0 cm<sup>-1</sup>, from ref 66. F<sub>1</sub>(<sup>3</sup>/<sub>2</sub>) term for OH X<sup>2</sup>Π<sub>3/2</sub> is -38.19 cm<sup>-1</sup>, based on data from ref 40. <sup>h</sup> Net Born–Oppenheimer diagonal corrections obtained at the CASSCF(7,2)/aug-cc-pVTZ level of theory: BODC = 602.3 (H<sub>2</sub>O), 640.9 (OH + H), 638.6 (O+2H) cm<sup>-1</sup> (using atomic masses). <sup>i</sup> From generally accepted values for  $\Delta H_{\text{f0}}^{\circ}(\text{H}_2\text{O})$ ,  $\Delta H_{\text{f0}}^{\circ}(\text{O})$ , and  $\Delta H_{\text{f0}}^{\circ}(\text{H})$ , see ref 8 for details. <sup>j</sup> IE(O) = 109837.02 ± 0.06 cm<sup>-1</sup> = 13.61806 eV, from Moore, C. E. *Ionization Potentials and Ionization Limits Derived from the Analyses of Optical Spectra*. Natl. Stand. Ref. Data Ser.—U.S. Natl. Bur. Stand. 34; U. S. Department Commerce: Washington, DC, 1970. <sup>k</sup> IE(OH) = 104989 ± 2 cm<sup>-1</sup>, ref 30. <sup>l</sup> Recommended experimental value from present study. <sup>m</sup> Based on  $D_0(\text{OH}) = 35420 \pm 15$  cm<sup>-1</sup> from Carlone and Dalby,<sup>15</sup> adopted as  $\Delta H_{\text{f0}}^{\circ}(\text{OH}) = 9.347 \pm 0.048$  kcal/mol in Gurvich et al.<sup>1</sup> <sup>n</sup> Based on  $\Delta H_{\text{f0}}^{\circ}(\text{OH}) = 9.17_5 \pm 0.29$  kcal/mol in JANAF<sup>3</sup> and NIST-JANAF.19. <sup>o</sup> Based on  $D_0(\text{H}-\text{OH}) = 41151 \pm 5$  cm<sup>-1</sup> from Rydberg tagging experiment 63.

proposed earlier in this study. If results only up to 6- $\zeta$  were to be considered, this dissociation energy would be underestimated by just 0.11 kcal/mol. Another very high-level theoretical treatment of  $D_0(\text{OH})$  by Martin obtained essentially the same value.<sup>117</sup> Although the theoretical value for  $D_0(\text{H}-\text{OH})$  is higher than the proposed experimental value by 0.17 kcal/mol, when taken together with the result for  $D_0(\text{OH})$ , neither the results of Carlone and Dalby<sup>15</sup> nor those listed in JANAF<sup>3,19</sup> seem plausible. Not only do the differences for  $D_0(\text{OH})$  exceed several times the implied uncertainty of the calculations, but in both cases, the calculated  $D_0(\text{OH})$  is *higher* than the spectroscopically determined bond energy. The latter would imply that the calculation seriously overestimates the total electronic energy of OH, which appears unlikely.

Hence, the theoretical results discussed above corroborate the currently recommended values for  $D_0(\text{H}-\text{OH})$  and  $D_0(\text{OH})$ . The calculations show unprecedented agreement with other relevant quantities as well (Table 5). For example, the value for  $\text{AE}_0(\text{OH}^+/\text{H}_2\text{O}) = 18.123$  eV that can be obtained directly from the computed quantities and has an estimated uncertainty of ±25 meV, is only 7 meV higher than the experimental consensus of  $18.116_2 \pm 0.003_0$  eV presented earlier. Another view on the benchmark enthalpy of atomization of H<sub>2</sub>O is provided through the equivalent enthalpy of formation of water. Aided by experimental enthalpies of formation of H and O, the calculation produces  $\Delta H_{\text{f0}}^{\circ}(\text{H}_2\text{O}) = -57.29 (\pm 0.30)$  kcal/mol, to be compared with the experimental value of  $-57.10 \pm 0.01$  kcal/mol. The calculated  $\Delta H_{\text{f0}}^{\circ}(\text{OH}) = 8.85 (\pm 0.18)$  kcal/mol that can be obtained in a similar fashion is identical to the experimental value proposed here, whereas the calculated  $\Delta H_{\text{f0}}^{\circ}(\text{OH}^+) = 309.00 (\pm 0.27)$  kcal/mol differs by only 0.03 kcal/mol. This level of theoretical accuracy is attainable because these calculations are the most sophisticated ever performed for OH and H<sub>2</sub>O using standard Gaussian basis set expansions and are among the most rigorous calculations ever performed for any molecule larger than H<sub>2</sub>.

## 5. Consequences

On the basis of the current photoionization results, the recommended values are  $D_0(\text{H}-\text{OH}) = 117.59 \pm 0.07$  kcal/mol,  $D_0(\text{OH}) = 101.76 \pm 0.07$  kcal/mol, and  $\Delta H_{\text{f0}}^{\circ}(\text{OH}) = 8.85 \pm 0.07$  kcal/mol. The equivalent 298 K values are given in Table 5. The new values proposed here produce a ripple effect that propagates throughout the thermochemical table, and its full assessment would require the individual examination of every entry in such a table. Here we will limit our discussion only to a few more obvious consequences.

For example, the enthalpy of deprotonation of water,  $\Delta H_{\text{acid0}}^{\circ}(\text{H}_2\text{O})$ , corresponding to the threshold for photoion-pair formation,  $\Delta H_{\text{f0}}^{\circ}(10)$



can be expressed as  $\Delta H_{\text{acid0}}^{\circ}(\text{H}_2\text{O}) = D_0(\text{H}-\text{OH}) + \text{IE}(\text{H}) - \text{EA}(\text{OH})$ , where EA stands for electron affinity. Using the accurate value<sup>118</sup> of  $\text{EA}(\text{OH}) = 14741.02 \pm 0.03$  cm<sup>-1</sup> produces  $\Delta H_{\text{acid0}}^{\circ}(\text{H}_2\text{O}) = 389.03 \pm 0.07$  kcal/mol ( $16.870_0 \pm 0.003_0$  eV) (cf. to  $390.7 \pm 0.1$  kcal/mol, listed by the WebBook<sup>119</sup>). Using enthalpy increments and entropies from Gurvich et al.,<sup>1</sup> the related gas-phase acidity of water is  $\Delta G_{\text{acid298}}^{\circ}(\text{H}_2\text{O}) = 383.61 \pm 0.07$  kcal/mol (cf. to listed<sup>119</sup> value  $384.1 \pm 0.2$  kcal/mol). Similarly, the enthalpy of deprotonation of hydroxyl,  $\Delta H_{\text{acid0}}^{\circ}(\text{OH}) = \Delta H_{\text{r0}}^{\circ}(11)$



is  $\Delta H_{\text{acid0}}^{\circ}(\text{OH}) = D_0(\text{OH}) + \text{IE}(\text{H}) - \text{EA}(\text{O})$ , and with<sup>120</sup>  $\text{EA}(\text{O}) = 11784.65 \pm 0.35$  cm<sup>-1</sup>, one obtains  $\Delta H_{\text{acid0}}^{\circ}(\text{OH}) = 381.66 \pm 0.07$  kcal/mol ( $16.550_3 \pm 0.003_2$  eV) and  $\Delta G_{\text{acid298}}^{\circ}(\text{OH}) = 376.69 \pm 0.07$  kcal/mol. The proton affinity of O,  $\text{PA}(\text{O}) = -\Delta H_{\text{r298}}^{\circ}(12)$



**TABLE 5: Summary of Calculated and Recommended Experimental Thermochemical Values<sup>a</sup>**

	current theoretical value	recommended experimental value
AE <sub>0</sub> (OH <sup>+</sup> /H <sub>2</sub> O)	18.123 (± 0.025) eV	18.116 <sub>2</sub> ± 0.003 <sub>0</sub> eV
IE(OH)	13.016 (± 0.003) eV	13.017 <sub>0</sub> ± 0.000 <sub>2</sub> eV <sup>b</sup>
D <sub>0</sub> (H–OH)	117.76 (± 0.15) kcal/mol	117.59 ± 0.07 kcal/mol
D <sub>298</sub> (H–OH)	–	118.81 ± 0.07 kcal/mol
D <sub>0</sub> (OH)	101.77 (± 0.12) kcal/mol	101.76 ± 0.07 kcal/mol
D <sub>298</sub> (OH)	–	102.75 ± 0.07 kcal/mol
ΔH <sub>f</sub> <sup>0</sup> (H <sub>2</sub> O)	–57.29 (± 0.30) kcal/mol	–57.10 ± 0.01 kcal/mol <sup>c</sup>
ΔH <sub>f</sub> <sup>0</sup> <sub>298</sub> (H <sub>2</sub> O)	–	–57.80 ± 0.01 kcal/mol <sup>c</sup>
ΔH <sub>f</sub> <sup>0</sup> (OH)	8.85 (± 0.18) kcal/mol	8.85 ± 0.07 kcal/mol
ΔH <sub>f</sub> <sup>0</sup> <sub>298</sub> (OH)	–	8.91 ± 0.07 kcal/mol
ΔH <sub>f</sub> <sup>0</sup> (OH <sup>+</sup> )	309.00 (± 0.27) kcal/mol	309.03 ± 0.07 kcal/mol
ΔH <sub>f</sub> <sup>0</sup> (OH <sup>+</sup> )	–	309.04 ± 0.07 kcal/mol
ΔH <sub>acid</sub> <sup>0</sup> <sub>298</sub> (OH)	–	389.03 ± 0.07 kcal/mol <sup>d</sup>
ΔH <sub>acid</sub> <sup>0</sup> <sub>298</sub> (OH)	–	390.20 ± 0.07 kcal/mol
ΔG <sub>acid</sub> <sup>0</sup> <sub>298</sub> (OH)	–	383.61 ± 0.07 kcal/mol
ΔH <sub>acid</sub> <sup>0</sup> (OH)	–	381.66 ± 0.07 kcal/mol <sup>e</sup>
ΔH <sub>acid</sub> <sup>0</sup> <sub>298</sub> (OH)	–	382.60 ± 0.07 kcal/mol
ΔG <sub>acid</sub> <sup>0</sup> (OH)	–	376.69 ± 0.07 kcal/mol
PA(O)	–	116.21 ± 0.07 kcal/mol <sup>b</sup>
GB(O)	–	109.99 ± 0.07 kcal/mol
PA(OH)	–	141.43 ± 0.07 kcal/mol <sup>f</sup>
GB(OH)	–	134.49 ± 0.07 kcal/mol
ΔH <sub>r</sub> <sup>0</sup> (CO + OH → CO <sub>2</sub> + H)	–	–23.98 ± 0.09 kcal/mol <sup>g</sup>
ΔH <sub>r</sub> <sup>0</sup> <sub>298</sub> (CO + OH → CO <sub>2</sub> + H)	–	–24.44 ± 0.09 kcal/mol
ΔH <sub>r</sub> <sup>0</sup> (CH <sub>2</sub> , a <sup>1</sup> A <sub>1</sub> + H <sub>2</sub> O → CH <sub>3</sub> + OH)	–	–0.38 ± 0.21 kcal/mol <sup>h</sup>
ΔH <sub>r</sub> <sup>0</sup> <sub>298</sub> (CH <sub>2</sub> , a <sup>1</sup> A <sub>1</sub> + H <sub>2</sub> O → CH <sub>3</sub> + OH)	–	–0.54 ± 0.21 kcal/mol
D <sub>0</sub> (CH <sub>3</sub> –OH)	–	90.15 ± 0.17 kcal/mol <sup>i</sup>
D <sub>298</sub> (CH <sub>3</sub> –OH)	–	92.00 ± 0.17 kcal/mol

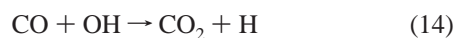
<sup>a</sup> All values are from the current study, unless otherwise noted. Enthalpy increments and entropies (for conversions to ΔH<sub>298</sub><sup>0</sup> and ΔG<sub>298</sub><sup>0</sup>) are from refs 1 and 2. <sup>b</sup> IE(OH) from ref 30. <sup>c</sup> From ref 2. See also ref 1, 3, and 8. <sup>d</sup> ΔH<sub>acid0</sub><sup>0</sup>(H<sub>2</sub>O) = ΔH<sub>r0</sub><sup>0</sup>(H<sub>2</sub>O → H<sup>+</sup> + OH<sup>–</sup>) = D<sub>0</sub>(H–OH) + EI(H) – EA(OH); EA(OH) is from ref 118. <sup>e</sup> ΔH<sub>acid0</sub><sup>0</sup>(OH) = ΔH<sub>r0</sub><sup>0</sup>(OH → H<sup>+</sup> + O<sup>–</sup>) = D<sub>0</sub>(OH) + EI(H) – EA(O); EA(O) is from ref 120. <sup>f</sup> IE(H<sub>2</sub>O) from ref 123. <sup>g</sup> ΔH<sub>r0</sub><sup>0</sup>(CO) = –27.20 ± 0.04 kcal/mol and ΔH<sub>r0</sub><sup>0</sup>(CO<sub>2</sub>) = –93.96 ± 0.03 kcal/mol from refs 1 and 2. <sup>h</sup> ΔH<sub>r0</sub><sup>0</sup>(CH<sub>2</sub>, a<sup>1</sup>A<sub>1</sub> + H<sub>2</sub>O → CH<sub>3</sub> + OH) = D<sub>0</sub>(H–OH) – D<sub>0</sub>(CH<sub>3</sub> to a<sup>1</sup>A<sub>1</sub> CH<sub>2</sub>). D<sub>0</sub>(CH<sub>3</sub> to a<sup>1</sup>A<sub>1</sub> CH<sub>2</sub>) = 117.97 ± 0.20 kcal/mol from ref 128. Alternatively, ΔH<sub>r0</sub><sup>0</sup>(CH<sub>2</sub>, a<sup>1</sup>A<sub>1</sub>) = 102.21 ± 0.20 kcal/mol and ΔH<sub>r0</sub><sup>0</sup>(CH<sub>3</sub>) = 35.86 ± 0.07 kcal/mol, also from ref 128. <sup>i</sup> ΔH<sub>r0</sub><sup>0</sup>(CH<sub>3</sub>OH) = –45.44 ± 0.14 kcal/mol from ref 1.

can be readily obtained through ΔH<sub>r0</sub><sup>0</sup>(11) = IE(OH) – D<sub>0</sub>(OH) – IE(H) and is PA(O) = 116.21 ± 0.07 kcal/mol (to be compared to listed value<sup>121,122</sup> 116.0 kcal/mol). The related gas-phase basicity of O, GB(O) = ΔG<sub>r298</sub><sup>0</sup>(12), is 109.99 ± 0.07 kcal/mol. The proton affinity of OH, PA(OH) = –ΔH<sub>r298</sub><sup>0</sup>(13)

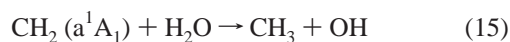


relates to ΔH<sub>r0</sub><sup>0</sup>(13) = IE(OH) – D<sub>0</sub>(H–OH) – IE(H) and is PA(OH) = 141.43 ± 0.07 kcal/mol, if one uses the accurate value<sup>123</sup> IE(H<sub>2</sub>O) = 101766 ± 2 cm<sup>–1</sup> (cf. to listed PA value<sup>121,122</sup> of 141.8 kcal/mol).

Of course, the reaction enthalpy (as calculated from available enthalpies of formation) for any chemical reaction in which the O–H bond in water or OH is either formed or destroyed changes when the new values for D<sub>0</sub>(H<sub>2</sub>O), D<sub>0</sub>(OH), or ΔH<sub>f</sub><sup>0</sup>(OH) are introduced. There are many possible examples that can be given here. For instance, the overall exothermicity for the important reaction 14 (which is a major oxidation pathway from CO to CO<sub>2</sub> and energy-releasing step in combustion and is also responsible for vernal and aestival cleaning of the atmosphere)



becomes slightly lower than previously thought, ΔH<sub>r0</sub><sup>0</sup>(14) = –23.98 ± 0.09 kcal/mol (cf. to previous best available value<sup>124</sup> of –24.48 kcal/mol) and ΔH<sub>r298</sub><sup>0</sup>(14) = –24.44 ± 0.09 kcal/mol. Another quite interesting reaction is



Because this reaction is very close to being thermoneutral, its

exo- or endothermicity changes with any change of the enthalpy of formation of CH<sub>2</sub> but also that of OH. The enthalpy of reaction can be expressed as ΔH<sub>r0</sub><sup>0</sup>(15) = D<sub>0</sub>(H–OH) – D<sub>0</sub>(H–CH<sub>2</sub> to CH<sub>2</sub> a<sup>1</sup>A<sub>1</sub>) = D<sub>0</sub>(H–OH) – D<sub>0</sub>(H–CH<sub>2</sub>) – ΔE(CH<sub>2</sub>, a<sup>1</sup>A<sub>1</sub> → X<sup>3</sup>B<sub>1</sub>). A number of combustion mechanisms appear to require this reaction to be exothermic.<sup>125,126</sup> We have recently determined a new accurate value<sup>127,128</sup> for the C–H bond dissociation energy in methyl radical D<sub>0</sub>(H–CH<sub>2</sub>) = 108.95 ± 0.20 kcal/mol (forming the ground-state triplet methylene) and hence 117.97 ± 0.20 kcal/mol to form singlet methylene, as well as ΔH<sub>r0</sub><sup>0</sup>(CH<sub>2</sub>) = 93.18 ± 0.20 kcal/mol. These values, together with the previous best available D<sub>0</sub>(H–OH) produced an enthalpy of reaction of 0.11 ± 0.20 kcal/mol, implying that the reaction is thermoneutral or perhaps even slightly endothermic. However, with the present value for D<sub>0</sub>(H–OH), this becomes once again slightly exothermic, ΔH<sub>r0</sub><sup>0</sup>(14) = –0.38 ± 0.21 kcal/mol, further increasing to –0.54 ± 0.21 kcal/mol at 298 K.

## 6. Conclusion

Several photoionization experiments utilizing the positive ion cycle to derive the O–H bond energy converge to a consensus value of AE<sub>0</sub>(OH<sup>+</sup>/H<sub>2</sub>O) = 146117 ± 24 cm<sup>–1</sup> (18.116<sub>2</sub> ± 0.003<sub>0</sub> eV). With the most accurate currently available ZEKE value<sup>30</sup> IE(OH) = 104989 ± 2 cm<sup>–1</sup>, corroborated by a number of photoelectron measurements,<sup>26–29</sup> this leads to D<sub>0</sub>(H–OH) = 41128 ± 24 cm<sup>–1</sup> = 117.59 ± 0.07 kcal/mol. This corresponds to ΔH<sub>r0</sub><sup>0</sup>(OH) = 8.85 ± 0.07 kcal/mol and implies D<sub>0</sub>(OH) = 35593 ± 24 cm<sup>–1</sup> = 101.76 ± 0.07 kcal/mol. The most sophisticated theoretical calculations performed so far on the H<sub>x</sub>O system, CCSD(T)/aug-cc-pVnZ, n = Q, 5, 6, and 7, extrapolated to the CBS limit and including corrections for core-

valence effects, scalar relativistic effects, incomplete correlation recovery, and diagonal Born–Oppenheimer corrections reproduce the experimental results to within 0.0–0.2 kcal/mol.

The new values of the two successive bond dissociation energies of water supersede the previously accepted values,<sup>1,3</sup> which were based on spectroscopic determinations<sup>15,16</sup> of  $D_0(\text{OH})$  using a very short Birge–Sponer extrapolation on  $\text{OH}/\text{OD } A^1\Sigma^+$ . An exhaustive analysis of the latter approach, combined with the application of the same procedure on a calculated potential energy curve for the state in question, demonstrates that the Birge–Sponer extrapolation underestimates the bond dissociation energy, although only the last vibrational level was not observed experimentally.

The new values affect a large number of other thermochemical quantities which directly or indirectly rely on or refer to  $D_0(\text{H–OH})$ ,  $D_0(\text{OH})$ , or  $\Delta H_f^\circ(\text{OH})$ .

These results of course also effect the thermochemistry of  $\text{D}_2\text{O}$ . However, at the level of accuracy reported here, this thermochemistry will require careful consideration of the mass-dependent Born–Oppenheimer correction which gives rise to the electronic isotope shift. This will be the subject of a future publication.

**Acknowledgment.** The work at Argonne National Laboratory (ANL) was supported by the U.S. Department of Energy, Office of Basic Energy Sciences, Division of Chemical Sciences under Contract No. W-31-109-ENG-38. The work at Pacific Northwest National Laboratory (PNNL) was supported by the U.S. Department of Energy, Office of Basic Energy Sciences, Divisions of Chemical Sciences and Biological and Environmental Research under Contract No. DE-AC06-76RLO 1830. The work at Lawrence Berkeley National Laboratory (LBNL) was supported by the U.S. Department of Energy, Office of Basic Energy Sciences, Division of Chemical Sciences under Contract No. DE-AC03-76SF00098. The work at Ames Laboratory was supported by the U.S. Department of Energy, Office of Basic Energy Sciences, Division of Chemical Sciences under Contract No. W-7405-Eng-82. Part of this research was performed in the William R. Wiley Environmental Molecular Sciences Laboratory (EMSL) at the PNNL. The EMSL is a national user facility funded by the Office of Biological and Environmental Research in the U.S. Department of Energy. PNNL, ANL, LBNL, and Ames Laboratory are multiprogram national laboratories operated by Battelle Memorial Institute (PNNL), University of Chicago (ANL), University of California Berkeley (LBNL), and Iowa State University (Ames Lab) for the U.S. Department of Energy.

#### Note Added in Proof

After this manuscript had been submitted, it came to our attention that at least two groups have further examined our original suggestion<sup>13</sup> that  $\Delta H_f^\circ(\text{OH})$  is too high by  $\sim 0.5$  kcal/mol.

Herbon et al. have recently submitted a paper<sup>129</sup> in which they supplement our findings with their observations that under certain conditions kinetic models consistently appear to underpredict the OH concentration. This led them to perform a carefully designed kinetic experiment from which they obtain  $\Delta H_{f0}^\circ(\text{OH}) = 8.86 \pm 0.16$  kcal/mol, providing an independent corroboration of the value of  $8.85 \pm 0.07$  kcal/mol reported here.

A recent paper by Joens<sup>130</sup> also follows up on our original letter.<sup>13</sup> From an analysis of available data, he reports  $\Delta H_{f0}^\circ(\text{OH}) = 8.88 \pm 0.03$  kcal/mol as an average of two

possible paths that appear to differ by only 0.03 kcal/mol: one is from  $\text{H}_2\text{O}$  and the other is from  $\text{H}_2\text{O}_2$ . The former utilizes the recent result on  $D_0(\text{H–OH})$  of Harich et al.,<sup>63</sup> and the latter utilizes the available literature value<sup>131</sup> of  $D_0(\text{HO–OH})$ . One of the major points of the contribution by Jones is not only that his proposed value is very similar to ours<sup>13</sup> but also that his apparent error bar is lower. Although the average value of Jones indeed appears to be extremely close to ours, we do not quite agree with several aspects of his approach, which bear directly on his reported error bar and, to some extent, on his reported value. For example, the  $D_0(\text{H–OH})$  value used in Joen's derivation and attributed to Harich et al. appears to be in error, because it is  $10 \text{ cm}^{-1}$  lower than that actually given by those authors. With the value as given by Harich et al., the difference between the two approaches averaged by Jones increases to 0.06 kcal/mol, tending to vitiate his quoted error bar. In addition, a more prudent approach requires that the value of Harich et al. be considered in a wider context, as discussed in section 2.3 on the present paper. Another important point is that the derivation of  $\Delta H_f^\circ(\text{OH})$  from  $D_0(\text{HO–OH})$  by necessity involves the enthalpy of formation of  $\text{H}_2\text{O}_2$ , which is established much less firmly than the enthalpy of formation of water. As mentioned in the present paper,<sup>8</sup> all major compilations report identical values for the enthalpy of water, which has been additionally verified through constant use. To the contrary, the much more seldom used values for  $\Delta H_{f298}^\circ(\text{H}_2\text{O}_2)$  found in the JANAF tables<sup>3,19</sup> and in the generally more careful compilation of Gurvich et al.<sup>1</sup> differ by slightly more than 0.05 kcal/mol. This alone makes somewhat suspect the nominal error bar of  $\pm 0.05$  kcal/mol attached to this quantity by Joens (JANAF tables do not report an error bar at all). The fact that the JANAF tables and Gurvich et al. appear to quote 0 K values that are slightly less disparate (0.02 kcal/mol) arises primarily from the fact that the JANAF tables obtain the 0 K value (used by Jones) through an enthalpy increment that does not properly account for the hindered rotation of  $\text{H}_2\text{O}_2$ . The parallel path to  $\Delta H_f^\circ(\text{OH})$  through  $\text{H}_2\text{O}_2$  is best analyzed through the use of a local thermochemical network,<sup>20,128,132</sup> which will be the subject of a future note.

#### References and Notes

- (1) Gurvich, L. V.; Veyts, I. V.; Alcock, C. B. *Thermodynamic Properties of Individual Substances*; Hemisphere: New York, 1989; Vol. 1.
- (2) Cox, J. D.; Wagman, D. D.; Medvedev, V. A. *CODATA Key Values for Thermodynamics*; Hemisphere: New York, 1989.
- (3) Chase, M. W., Jr.; Davies, C. A.; Downey, J. R., Jr.; Frurip, D. J.; McDonald, R. A.; Syverud, A. N. JANAF Thermochemical Tables, 3rd ed. *J. Phys. Chem. Ref. Data* **1985**, *14*, Suppl. 1.
- (4) Herzberg, G. *J. Mol. Spectrosc.* **1970**, *33*, 147.
- (5) Brix, P.; Herzberg, G. *Can. J. Phys.* **1954**, *32*, 110.
- (6) King, R. C.; Armstrong, G. T. *J. Res. NBS.* **1968**, *72A*, 113. See also: Rossini, F. D. *J. Res. NBS* **1939**, *22*, 407. Rossini, F. D. *J. Res. NBS* **1931**, *6*, 1.
- (7) Haar, L.; Gallagher, J. S.; Kell, G. G. *NBS–NRC Steam Tables*; Hemisphere: New York, 1983.
- (8)  $\Delta H_{f0}^\circ(\text{H}) = 51.6337 \pm 0.0014$  kcal/mol,  $\Delta H_{f0}^\circ(\text{O}) = 58.984 \pm 0.021$  kcal/mol, and  $\Delta H_{f0}^\circ(\text{H}_2\text{O}) = -57.104 \pm 0.010$  kcal/mol are used here. These values are identical in all three major compilations: Gurvich et al.,<sup>1</sup> CODATA,<sup>2</sup> and JANAF,<sup>3</sup> because they are based on the same experimental measurements. Gas-phase  $\text{H}_2$  and  $\text{O}_2$  are reference states, and hence  $\Delta H_{f0}^\circ(\text{H}) = \frac{1}{2}D_0(\text{H}_2)$  and  $\Delta H_{f0}^\circ(\text{O}) = \frac{1}{2}D_0(\text{O}_2)$ . The selected<sup>1–3</sup> enthalpies of formation of H and O are based on  $D_0(\text{H}_2) = 36118.3 \pm 1 \text{ cm}^{-1}$  from Herzberg,<sup>4</sup> and  $D_0(\text{O}_2) = 41260 \pm 15 \text{ cm}^{-1}$  from Brix and Herzberg.<sup>5</sup> The path leading to  $\Delta H_{f0}^\circ(\text{H}_2\text{O}, \text{g})$  is slightly more complicated. Measurements<sup>6</sup> of combustion of  $\text{H}_2$  in  $\text{O}_2$  provide the 298 K enthalpy of formation of liquid water,  $\Delta H_{f298}^\circ(\text{H}_2\text{O}, \text{l}) = -68.315 \pm 0.010$  kcal/mol. This quantity is combined with the 298 K enthalpy of vaporization,  $\Delta H_{\text{vap}298}^\circ(\text{H}_2\text{O}, \text{l}) = 10.5172 \pm 0.0005$  kcal/mol (from steam tables, Haar et al.<sup>7</sup>) to give the gas-phase enthalpy of formation at 298 K,  $\Delta H_{f298}^\circ(\text{H}_2\text{O}, \text{g}) = -57.798 \pm 0.010$  kcal/mol. The 0 K enthalpy of formation of water,



$\Delta H_{0}^{\circ}(\text{H}_2\text{O}, \text{g}) = -57.104 \pm 0.010$  kcal/mol, can be obtained from 298 K value with the aid of enthalpy increments ( $\Delta H_{298}^{\circ} - \Delta H_0^{\circ}$ ) for  $\text{H}_2$  (2.0239  $\pm$  0.0002 kcal/mol),  $\text{O}_2$  (2.0746  $\pm$  0.0005 kcal/mol), and  $\text{H}_2\text{O}(\text{g})$  (2.3674  $\pm$  0.0012 kcal/mol), which were calculated<sup>2</sup> by direct summation of states.

(9) Spectroscopic (0 K) values for bond dissociation energies, as well as 0 K values for other thermochemical quantities are used throughout this paper. Chemists most often use 298 K values, which can be easily obtained from the 0 K values and the appropriate enthalpy increments ( $H_{298} - H_0$ ) of all the species involved. For the readers' convenience, the following conversions are given explicitly here:  $D_{298}(\text{H}-\text{OH}) = D_0(\text{H}-\text{OH}) + 1.220$  kcal/mol,  $D_{298}(\text{OH}) = D_0(\text{OH}) + 0.982$  kcal/mol,  $\Delta H_{298}^{\circ}(\text{OH}) = \Delta H_0^{\circ}(\text{OH}) + 0.057$  kcal/mol.

(10) The following conversion factors have been used in this paper: 1 eV = 8065.545  $\text{cm}^{-1}$  = 23.06055 kcal/mol, 1 H = 27.2113834 eV = 219474.631  $\text{cm}^{-1}$  = 627.5095 kcal/mol, and 1 kcal/mol = 4.184 kJ/mol = 349.755  $\text{cm}^{-1}$ , all based on the 1998 CODATA recommended values of fundamental physical constants: Mohr, P. J.; Taylor, B. N. *J. Phys. Chem. Ref. Data* **1999**, *28*, 7013. See also: Mohr, P. J.; Taylor, B. N. *Rev. Mod. Phys.* **2000**, *72*, 351.

(11) The reader should be reminded that enthalpies of formation are always derived quantities, deduced from experimental measurements that correspond to thermochemical changes involving several species, such as enthalpies of reactions, bond dissociation energies, etc. In this case,  $\Delta H_0^{\circ}(\text{OH})$  can be deduced either from a measurement of  $D_0(\text{H}-\text{OH})$  or  $D_0(\text{OH})$ , or, at least in principle, from any other chemical reaction involving OH (assuming that the thermochemical properties of other species that are involved in the same reaction are known independently of OH and with sufficient accuracy).

(12) In fact, one can simply show that the enthalpy of formation of OH directly relates to the difference between the first and second bond dissociation energy of water:  $\Delta H_0^{\circ}(\text{OH}) = \{[D_0(\text{H}-\text{OH}) - D_0(\text{OH})] + [D_0(\text{H}_2) + D_0(\text{O}_2) - \Delta H_{\text{atomiz}0}^{\circ}(\text{H}_2\text{O})]\}/2 = [D_0(\text{H}-\text{OH}) - D_0(\text{OH})]/2 + 0.940 \pm 0.022$  kcal/mol.

(13) Ruscic, B.; Feller, D.; Dixon, D. A.; Peterson, K. A.; Harding, L. B.; Asher, R. L.; Wagner, A. F. *J. Phys. Chem. A* **2001**, *105*, 1.

(14) Berkowitz, J.; Ellison, G. B.; Gutman, D. *J. Phys. Chem.* **1994**, *98*, 2744.

(15) Carlone, C.; Dalby, F. W. *Can. J. Phys.* **1969**, *47*, 1945.

(16) Barrow, R. F. *Ark. Fys.* **1956**, *11*, 281.

(17) In the discussion found in the 3rd edition of the JANAF Tables,<sup>3</sup> the authors state: "A value of  $\Delta H_0^{\circ}(\text{OH}) = 35450 \pm 100$   $\text{cm}^{-1}$  = 101.356  $\pm$  0.29 kcal/mol was adopted ... one obtains  $\Delta_f H^{\circ}(\text{OH}, \text{g}, 0 \text{ K}) = 9.261 \pm 0.29$  kcal/mol, which is in good agreement with the last JANAF selection", namely  $\Delta H_0^{\circ}(\text{OH}) = 9.29 \pm 0.3$  kcal/mol from the 2nd edition (Stull, D. R.; Prophet, H. *JANAF Thermochemical Tables*, 2nd ed., NSRDS-NBS 37; U.S. Gov. Printing Office: Washington, DC, 1971). The value in the 2nd edition is nominally based on same determination by Barrow<sup>16</sup> that was used in the 3rd edition, but for some reason the adopted  $D_0(\text{OH})$  was 35440  $\pm$  100  $\text{cm}^{-1}$  in the 2nd edition.

(18) The OH data in JANAF<sup>3</sup> is afflicted by a number of additional inaccuracies. The most serious is an incorrect treatment of the degeneracy and multiplicity of the ground electronic state of OH, resulting in large errors in the calculated heat capacity and enthalpy increments.

(19) Chase, M. W., Jr. NIST-JANAF Thermochemical Tables, 4th ed. *J. Phys. Chem. Ref. Data* **1998**, Monograph No. 9.

(20) Ruscic, B. *Res. Adv. Chem. Phys.* **2000**, *1*, 36.

(21) The stationary electron convention is used for all ion thermochemistry, although in this case the distinction is purely academic, because the difference between the thermal electron convention and stationary electron convention vanishes at 0 K. It should be also noted that the equivalence between the fragment appearance energy and the enthalpy of the corresponding reaction is correct only at 0 K, regardless of the convention used. Hence,  $\Delta H_{298}^{\circ}(\text{ABC} \rightarrow \text{AB}^+ + \text{C} + \text{e}^-) \neq \text{AE}_{298}(\text{AB}^+/\text{ABC})$ , a frequent mistake encountered in the literature. Rather, it can be easily shown<sup>20</sup> that for a nonlinear polyatomic molecule ABC  $\Delta H_{298}^{\circ}(\text{ABC} \rightarrow \text{AB}^+ + \text{C} + \text{e}^-) = \text{AE}_{298}(\text{AB}^+/\text{ABC}) - \frac{5}{2}kT + (\Delta H_{298}^{\circ} - \Delta H_0^{\circ})(\text{AB}^+) + (H_{298}^{\circ} - H_0^{\circ})(\text{C})$ . However, it is easier to first correct  $\text{AE}_{298}$  to  $\text{AE}_0$  by applying the available internal energy of ABC,  $(\Delta H_{298}^{\circ} - \Delta H_0^{\circ})(\text{ABC}) - \frac{5}{2}kT$ , and then undertake the thermochemical arithmetics.

(22) Dibeler, V. H.; Walker, J. A.; Rosenstock, H. M. *J. Res. Natl. Bur. Stand.* **1966**, *70A*, 459.

(23) McCulloh, K. E. *Int. J. Mass Spectrom. Ion Phys.* **1976**, *21*, 333.

(24) Berkowitz, J.; Appelman, E. H.; Chupka, W. A. *J. Chem. Phys.* **1973**, *58*, 1950.

(25) The values of Dibeler et al.<sup>22</sup> and McCulloh<sup>23</sup> are based on the appearance energy of the  $\text{OH}^+$  fragment from water, whereas Berkowitz et al.<sup>24</sup> use the  $\text{OH}^+$  and  $\text{O}^+$  fragments from HOF. In all three cases, the photoionization measurements lead to a measure of the enthalpy of formation of  $\text{OH}^+$ . This was then combined with the tabulated enthalpy of formation of OH to produce  $\text{IE}(\text{OH})$ , which was the primary unknown at the time. However, most of the auxiliary thermochemical quantities used in the original estimations are now outdated. Assuming  $\Delta H_0^{\circ}(\text{OH}) = 9.3$  kcal/mol (as it was done by all three groups), but using the best current values<sup>1,2</sup>

for  $\Delta H_0^{\circ}(\text{HF})$ ,  $\Delta H_0^{\circ}(\text{F})$ ,  $\Delta H_0^{\circ}(\text{H}_2\text{O})$ , and  $\Delta H_0^{\circ}(\text{H})$ , the uncorrected threshold of Dibeler et al.<sup>22</sup> implies  $\text{IE}(\text{OH}) = 12.90$  eV, Berkowitz et al.<sup>24</sup> results in  $\geq 12.88$  eV, and McCulloh<sup>23</sup> results in 12.97 eV. Assuming a different value for  $\Delta H_0^{\circ}(\text{OH})$  changes accordingly the deduced  $\text{IE}(\text{OH})$ .

(26) Katsumata, S.; Lloyd, D. R. *Chem. Phys. Lett.* **1977**, *45*, 519.

(27) Dyke, J. M.; Jonathan, N.; Morris, A. *Electron Spectroscopy: Theory, Techniques and Applications*; Brundle, C. R., Baker, A. D., Eds.; Academic: New York, 1979; Vol. 3.

(28) Van Lonkhuyzen, H.; De Lange, C. A. *Mol. Phys.* **1984**, *51*, 551.

(29) Barr, J. D.; De Fanis, A.; Dyke, J. M.; Gamblin, S. D.; Hooper, N.; Morris, A.; Stranges, S.; West, J. B.; Wright, T. G. *J. Chem. Phys.* **1999**, *110*, 345.

(30) Wiedmann, R. T.; Tonkyn, R. G.; White, M. G. *J. Chem. Phys.* **1992**, *97*, 768.

(31) Berkowitz, J.; Gibson, S. T.; Ruscic, B. 1984, unpublished data.

(32) Dehmer, P. M. *Chem. Phys. Lett.* **1984**, *110*, 79.

(33) Cutler, J. N.; He, Z. X.; Samson, J. A. R. *J. Phys. B* **1995**, *28*, 4577.

(34) Berkowitz et al.<sup>14</sup> list the discrepancy between the two approaches as a curiosity, commenting that "the precise reason [for this] is not known".

(35) Birge, R. T.; Spomer, H. *Phys. Rev.* **1926**, *28*, 259.

(36) Herzberg, G. *Molecular Spectra and Molecular Structure I. Spectra of Diatomic Molecules*; Van Nostrand: New York, 1950.

(37) Gaydon, A. G. *Dissociation Energies and Spectra of Diatomic Molecules*, 3rd ed.; Chapman and Hall: London, 1968.

(38) Dunham, J. L. *Phys. Rev.* **1932**, *41*, 713. Dunham, J. L. *Phys. Rev.* **1932**, *41*, 726.

(39) Beckel, C. L.; Engelke, R. *J. Chem. Phys.* **1968**, *49*, 5199.

(40) Huber, K. P.; Herzberg, G. *Molecular Spectra and Molecular Structure. IV. Constants of Diatomic Molecules*; Van Nostrand: New York, 1979.

(41) Guyon, P. M.; Berkowitz, J. *J. Chem. Phys.* **1971**, *54*, 1814. Chupka, W. A. *J. Chem. Phys.* **1971**, *54*, 1936.

(42) Ruscic, B.; Berkowitz, J. *J. Phys. Chem.* **1993**, *97*, 11451. Ruscic, B.; Berkowitz, J. *J. Chem. Phys.* **1994**, *100*, 4498. Ruscic, B.; Berkowitz, J. *J. Chem. Phys.* **1994**, *101*, 7795. Ruscic, B.; Berkowitz, J. *J. Chem. Phys.* **1994**, *101*, 7975. Ruscic, B.; Berkowitz, J. *J. Chem. Phys.* **1994**, *101*, 10936. Asher, R. L.; Appelman, E. H.; Ruscic, B. *J. Chem. Phys.* **1996**, *105*, 9781. Asher, R. L.; Ruscic, B. *J. Chem. Phys.* **1997**, *106*, 210.

(43) The veracity of this statement is tested regularly, albeit indirectly, through the resulting bond energies and enthalpies of formation of radicals. However, a recent example provides a direct comparison of fragmentation onsets obtained by different methods. We have recently reported  $\text{AE}_0(\text{CH}_3^+/\text{CH}_4) = 14.322 \pm 0.003$  eV, which was obtained by fitting the  $\text{CH}_3^+$  fragment ion yield curve from methane at room temperature. (Litorja, M.; Ruscic, B. *J. Chem. Phys.* **1997**, *107*, 9852). Subsequently, a significantly more complex PFI-PEPICO study that was carried out using synchrotron light and jet-expansion-cooled methane reported 14.323  $\pm$  0.001 eV for the same threshold (Weitzel, K. M.; Malow, M.; Jarvis, G. K.; Baer, T.; Song, Y.; Ng, C. Y. *J. Chem. Phys.* **1999**, *111*, 8267).

(44) Weitzel, K. M.; Jarvis, G. K.; Malow, M.; Baer, T.; Song, Y.; Ng, C. Y. *Phys. Rev. Lett.* **2001**, *86*, 3526.

(45) Curtiss, L. A.; Raghavachari, K.; Trucks, G. W.; Pople, J. A. *J. Chem. Phys.* **1991**, *94*, 7221. Curtiss, L. A.; Raghavachari, K.; Redfern, P. C.; Pople, J. A. *J. Chem. Phys.* **1997**, *106*, 1063.

(46) Curtiss, L. A.; Raghavachari, K.; Redfern, P. C.; Rassolov, V.; Pople, J. A. *J. Chem. Phys.* **1998**, *109*, 7764.

(47) The quoted<sup>46</sup> "average absolute deviation" of G3 theory from the experiment is 1.02 kcal/mol, and the root-mean-square deviation is 1.45 kcal/mol. The error bar that would be commensurate to what is customarily quoted by an experimentalist ( $\sim 2$  standard deviations or  $\sim 98\%$  confidence limits) would then be  $\pm 2.9$  kcal/mol for G3 theory. For G2 theory, the average absolute deviation on the G2/97 set is 1.48 kcal/mol, the root-mean-square deviation is 1.93 kcal/mol, and hence the error bar corresponding to 2 standard deviations is  $\pm 3.8$  kcal/mol. Note also that the experimental enthalpy of formation of OH (9.4 kcal/mol) is a member of both the G2 and G2/97 training sets that were used to determine the higher level corrections for these theories.

(48) Dixon, D. A.; Feller, D.; Peterson, K. A. *J. Phys. Chem.* **1997**, *101*, 9405. Feller, D.; Dixon, D. A.; Peterson, K. A. *J. Phys. Chem.* **1998**, *102*, 7053. Dixon, D. A.; Feller, D. *J. Phys. Chem. A* **1998**, *102*, 8209. Feller, D.; Peterson, K. A. *J. Chem. Phys.* **1999**, *110*, 8384. Dixon, D. A.; Feller, D.; Sandrone, G. *J. Phys. Chem. A* **1999**, *103*, 4744. Feller, D.; Dixon, D. A. *J. Phys. Chem.* **1999**, *103*, 6413. Feller, D.; Peterson, K. A. *J. Chem. Phys.* **1998**, *108*, 154. Feller, D. *J. Comput. Chem.* **1996**, *17*, 1571. The database is available at URL: <http://www.emsl.pnl.gov:2080/proj/crdb/>.

(49) Purvis, G. D., III; Bartlett, R. J. *J. Chem. Phys.* **1982**, *76*, 1910. Raghavachari, K.; Trucks, G. W.; Pople, J. A.; Head-Gordon, M. *Chem. Phys. Lett.* **1989**, *157*, 479. Watts, J. D.; Gauss, J.; Bartlett, R. J. *J. Chem. Phys.* **1993**, *98*, 8718.

(50) Dunning, T. H., Jr. *J. Chem. Phys.* **1989**, *90*, 1007. Kendall, R. A.; Dunning, T. H., Jr.; Harrison, R. J. *J. Chem. Phys.* **1992**, *96*, 6796. Woon, D. E.; Dunning, T. H., Jr. *J. Chem. Phys.* **1995**, *103*, 4572.

(51) Litorja, M.; Ruscic, B. *J. Electron Spectrosc.* **1998**, *97*, 131.

(52) Partridge, H.; Schwenke, D. W. *J. Chem. Phys.* **1997**, *106*, 4618.

(53) A list of 170625 rovibrational levels for J up to 55 is available as Supporting Information to Reference 52. The energies have been obtained by solving the empirically corrected potential energy surface of the ground state of H<sub>2</sub>O, which was adjusted to reproduce correctly (generally within a very small fraction of a wavenumber) known experimental lines. The advantage of using the calculated energies is 2-fold. The list includes all levels, regardless of whether they are known experimentally or not. In addition, for every level, the listing provides unambiguous assignments via vibrational and rotational quantum numbers  $\nu_1, \nu_2, \nu_3, J, K_a$ , and  $K_c$  as well as nuclear symmetry, from which the necessary degeneracies (including the correct statistical weights for ortho and para water) can be trivially generated.

(54)  $\langle E \rangle_{\text{vib,rot}} = (\eta + 1)/\alpha$  (note that  $\alpha$  has units of inverse energy).

(55) In the past, we have often started the process of determining the "best" internal energy function by calculating the density of states through approximate (continuous) expressions,<sup>42</sup> such as that given by Haarhoff (Haarhoff, P. C.; *Mol. Phys.* **1963**, *7*, 101). For H<sub>2</sub>O, Haarhoff's function is a very poor starting distribution because it peaks at 0, rather than close to  $1/2kT$ , which would be expected from the three-rotor function. Hence, in the present case, it is much better to start from a direct state count, despite the disadvantage of a discrete (rather than continuous) state density. Luckily, the discrete count is easily obtained by simply using the known rotational and vibrational levels of the ground state of H<sub>2</sub>O.<sup>52,53</sup>

(56) Two properties of the internal energy distribution function are important in the present context: the behavior of its integral from a given starting internal energy to infinity and the expectation value of the internal energy. Hence, if we start from the three-rotor function, the two parameters in the assumed  $E^{\nu} \exp(-\alpha E)$  form of the desired function can be adjusted by least-squares fitting, where the fitted properties are the behavior of the integral in comparison to the analogous sum over the calculated discrete state count and the desired average internal energy.

(57) The shift is much smaller than what would be simplistically expected from the fwhm that reflects the experimental resolution, because it depends on the ratio of fwhm to the apparent width of the feature in question. In practice, the threshold region of the fragment ion yield curve shifts toward lower energy by a very small amount, mostly in the region immediately below the 0 K threshold.

(58) Heimann, P.; Koike, M.; Hsu, C. W.; Blank, D.; Yang, X.-M.; Suits, A.; Lee, Y. T.; Evans, M.; Ng, C. Y.; Flaim, C.; Padmore, H. A. *Rev. Sci. Instrum.* **1997**, *68*, 1945.

(59) Ng, C. Y. In *Photoionization and Photodetachment*; Ng, C. Y., Ed.; *Adv. Ser. Phys. Chem.*; World Scientific: Singapore, 2000; Vol. 10A, p 394.

(60) Jarvis, G. K.; Song, Y.; Ng, C. Y. *Rev. Sci. Instrum.* **1999**, *70*, 2615.

(61) Jarvis, G. K.; Weitzel, K.-M.; Malow, M.; Baer, T.; Song, Y.; Ng, C. Y. *Rev. Sci. Instrum.* **1999**, *70*, 3892.

(62) Stimson, S.; Chen, Y.-J.; Evans, M.; Liao, C.-L.; Ng, C. Y.; Hsu, C.-W.; Heimann, P. *Chem. Phys. Lett.* **1998**, *289*, 507.

(63) Harich, S. A.; Hwang, D. W. H.; Yang, X.; Lin, J. J.; Yang, X.; Dixon, R. N. *J. Chem. Phys.* **2000**, *113*, 10073.

(64) A Carlone and Dalby<sup>15</sup> report of  $\Delta G(v + 1/2)$  contains a typographical error for  $\Delta G(6.5)$  which should be 1558.3 cm<sup>-1</sup>.

(65) Dieke, G. H.; Crosswhite, H. M. *The Ultraviolet Bands of OH Fundamental Data*; Bumblebee Series Report No. 87, Johns Hopkins University: Baltimore, MD, 1948. See also: Dieke, G. H.; Crosswhite, H. M. *J. Quant. Spectrosc. Rad. Transfer* **1962**, *2*, 97. Also, Huber and Herzberg.<sup>40</sup>

(66) Moore, C. E. *Atomic Energy Levels*; NBS Circ 467, U.S. National Bureau of Standards: Washington, DC, 1949; Vol. 1.

(67) Carlone and Dalby<sup>15</sup> compare  $D_0(\text{OH}, A^2\Sigma^+)$  and  $D_0(\text{OD}, A^2\Sigma^+)$  as follows. Adding the  $P_1(1)$  transition<sup>65</sup> of 32440.6 cm<sup>-1</sup> to  $D_0(\text{OH}, A^2\Sigma^+) = 18847$  cm<sup>-1</sup>, they obtain the energy of the H(2S) + O(1D<sub>2</sub>) limit relative to X<sup>2</sup>Π<sub>3/2</sub>,  $J = 3/2, v = 0$  as 51287.6 cm<sup>-1</sup>. Starting from this value, they subtract  $D_0(\text{OD}, A^2\Sigma^+) = 19263$  cm<sup>-1</sup> and the energy of the  $P_1(1)$  transition in OD (32528.5 cm<sup>-1</sup>, Ishaq, M. *Proc. R. Soc. (London) Ser. A* **1937**, *159*, 110. See also Huber and Herzberg<sup>40</sup>), which produces the offset of the  $J = 3/2, v = 0$  level of X<sup>2</sup>Π<sub>3/2</sub> in OD relative to the same level in OH as -503.9 cm<sup>-1</sup>. They compare this value to the spectroscopic difference of the vibrational zero-point energies of OH and OD of -498.1 cm<sup>-1</sup> and attribute the residual difference of -5.8 cm<sup>-1</sup> to electronic isotope shifts. In fact, the best presently available difference in vibrational zero-point energies<sup>40</sup> of X<sup>2</sup>Π<sub>3/2</sub> of OH and OD, including the  $Y_{00}$  term but excluding the rotational terms, is -499.97 cm<sup>-1</sup>, even closer to their derived offset. However, because the offset of the lowest level of OD relative to OH of -498.1 cm<sup>-1</sup> is derived by using experimental  $P_1(1)$  values, rather than  $\nu_{00}$  (which would make it refer to the zero-point of the Hill-Van Vleck expression), it should really have been compared to the difference in zero-point energies that includes the  $F_1(3/2)$  terms.<sup>36,40</sup> When those are included, the expected difference is -513.46 cm<sup>-1</sup> leading to a residual discrepancy of 9.6 cm<sup>-1</sup>.

(68) The electronic energy of the hydrogen atom within the Born-Oppenheimer approximation is  $E_e(\text{H}) = m_e c^3 \mu_0 2e^4 / 8h^3 = 0.5$  Hartree = 109737.315 cm<sup>-1</sup>, where  $m_e$  is the rest mass of the electron,  $c$  is the speed of light in a vacuum,  $e$  is the elementary charge, and  $h$  is Planck constant. This solution corresponds to an infinite nuclear mass. Substitution of the proper reduced masses,  $\mu_e(\text{H}) = 0.999455975m_e$ , and  $\mu_e(\text{D}) = 0.999727704m_e$ , gives an isotope shift with the electron in D being more bound than in H by 29.8 cm<sup>-1</sup>. The electronic energy of other atoms and molecules calculated within the Born-Oppenheimer approximation has similar limitations, which unfortunately cannot be so readily corrected. In molecules, the whole potential energy curve, including the dissociation asymptote, is shifted upwards compared to the infinite nuclear mass result. The electronic isotope shift is the difference in the asymptotic upward shift from that at the bottom of the curve. For the ground electronic states of H<sub>2</sub><sup>+</sup>, HD<sup>+</sup>, and D<sub>2</sub><sup>+</sup>, Van Vleck (Van Vleck, J. H. *J. Chem. Phys.* **1936**, *4*, 327) found electronic isotope shifts of less than a wavenumber. However, for H<sub>2</sub>, HD, and D<sub>2</sub>, Van Vleck found larger shifts of 5.4, 4.6, and 2.8 cm<sup>-1</sup>, respectively, with the lighter isotope being more bound. The sign and magnitude of these shifts were confirmed by experimental findings of Herzberg and Monfils (Herzberg, G.; Monfils, A. *J. Mol. Spectrosc.* **1960**, *5*, 482). However, Kleinman and Wolfsberg (Kleinman, L. I.; Wolfsberg, M. *J. Chem. Phys.* **1973**, *59*, 2043) calculated the adiabatic portion of electronic isotope shifts for <sup>1</sup>Σ<sup>+</sup> states of several diatomic molecules HX/DX, with X = H, Li, B, N, and F. Except for H, they found negative electronic isotope shifts, corresponding to lighter isotopes being less bound by 1-15 cm<sup>-1</sup>, depending on X. In section 4, we present higher level but related calculations for the <sup>2</sup>Π<sub>3/2</sub> ground state of OH that also find slightly negative electronic isotope shifts, corresponding to lighter isotopes being less bound.

(69) Carlone and Dalby<sup>15</sup> report  $\Delta G(0.5) = 659.7$  cm<sup>-1</sup> in OH ( $B^2\Sigma^+$ ) and  $\Delta G(0.5) = 546.9$  cm<sup>-1</sup> and  $\Delta G(1.5) = 357.9$  cm<sup>-1</sup> in OD ( $B^2\Sigma^+$ ).

(70) Felenbock, P. *Ann. Astrophys.* **1963**, *5*, 393.

(71) The rotational constants given in ref 15, together with the Supporting Information containing lines for the B → A system (Depository of Unpublished Data, National Science Library, National Research Council of Canada, Ottawa, Canada), provide sufficient information to deduce the energies of the pertinent levels of OH B<sup>2</sup>Σ<sup>+</sup>. Relative to the rotationless level of  $v = 0$ , these are 1167.1 cm<sup>-1</sup> ( $v = 0, N = 15$ ), 1314.7 cm<sup>-1</sup> ( $v = 0, N = 16$ ), 1003.1 cm<sup>-1</sup> ( $v = 1, N = 9$ ), and 1067.1 cm<sup>-1</sup> ( $v = 1, N = 10$ ). Obviously, the energies of unobserved levels are estimated from constants inferred from the observed level. Note also that the constants for  $v = 1$  of the B state as given in Table 6 of ref 15 are wrong, and underestimate  $N = 9$  by 105 cm<sup>-1</sup>. The correct constants, obtained by fitting the available levels of  $v = 1$ , are  $B_1 = 4.085$  cm<sup>-1</sup>,  $D_1 = 0.937 \times 10^{-3}$  cm<sup>-1</sup>, and  $H_1 = -2.32 \times 10^{-5}$  cm<sup>-1</sup>.

(72) The reported<sup>15,69</sup>  $\Delta G(0.5)$  and  $\Delta G(1.5)$  values for OD are just sufficient to obtain  $\omega_e$  and  $\omega_e x_e$ . Using the isotopic relations  $\omega_e(\text{OH}) = f \times \omega_e(\text{OD})$  and  $\omega_e x_e(\text{OH}) = f^2 \times \omega_e x_e(\text{OD})$ , where  $f = 1.373465$  is the square root of the ratio of reduced masses of OD and OH, this closely reproduces  $\Delta G(0.5)$  of OH. Better yet, a least-squares fit of all three  $\Delta G(v + 1/2)$  values produces  $\omega_e(\text{OH}) = 1015.4$  cm<sup>-1</sup> and  $\omega_e x_e(\text{OH}) = 179.2$  cm<sup>-1</sup>.

(73)  $\nu_{00}$  of B<sup>2</sup>Σ<sup>+</sup> → A<sup>2</sup>Σ<sup>+</sup> in OH is 35965.5 cm<sup>-1</sup> (ref 40), and O(1S) is 17924.7 cm<sup>-1</sup> above O(1D) (ref 66). Hence,  $D_0(\text{OH}, B^2\Sigma^+) = D_0(\text{OH}, A^2\Sigma^+) - 18040.8$  cm<sup>-1</sup>.

(74) Our results differ from those of ref 15 within a few tenths of one wavenumber, most likely due to differences in round-off error.

(75) For example, simple summation of  $\Delta G$  values for the lowest (fourth) order polynomial fit for OH gives  $G(10) = 18862.5$  cm<sup>-1</sup> but an integrated  $D_0(\text{OH}, A^2\Sigma^+)$  of 18843.7 cm<sup>-1</sup>, or 15.6 cm<sup>-1</sup> less. Fifth and sixth order polynomials give similar results. For OD, the discrepancies are slightly less, amounting to 3.2 and 7.7 cm<sup>-1</sup>.

(76) The  $\Delta G(v + 1/2) \approx d[G(v)]/dv$  approximation can be trivially avoided if instead of eq 6 one uses the more convenient form:  $\Delta G(v + 1/2) = \sum b_j [(v + 3/2)^{j+1} - (v + 1/2)^{j+1}]$ ;  $j = 0, 2, \dots, n$ , where the coefficients  $b_j$ ,  $j = 0, 1, 2, 3, \dots$ , etc. correspond transparently to  $\omega_e, -\omega_e x_e, \omega_e y_e, \omega_e z_e$ , etc., producing straightforwardly expressions for both  $G(v)$  and  $d[G(v)]/dv$ , as well as providing the vibrational zero-point energy  $ZPE = G(0)$ , etc. This function is completely equivalent to that of eq 6. Once  $G(v)$  and its derivative  $d[G(v)]/dv$  are known,  $D_0$  implied by the fit is obtained by finding the maximum vibrational energy supported by the expression for  $G(v)$  and subtracting  $G(0)$ . The fractional vibrational quantum number for which  $G(v)$  achieves a maximum,  $\nu_{\text{max}}$ , has exactly the same meaning as and hence is directly comparable to  $(v + 1/2)_{\text{intercept}}$  obtained via the more traditional form of the Birge-Sponer fit.

(77) The corresponding  $\nu_{\text{max}}$  values, obtained as averages from three fits ( $n = 5, 6$ , and  $7$ ) are 9.964 for OH and 13.843 for OD, not very different from the  $(v + 1/2)_{\text{intercept}}$  values of ref 15 of 9.955 for OH and 13.836 for OD. The principal difference in the resulting  $D_0$  is not in the integration limit, but in the integrand.

(78) Differences in electronic isotope shifts of two states (as opposed to absolute shifts of any one particular state) can be readily obtained if sufficient experimental data is available. For example, let  $T_e(\text{OH}, A^2\Sigma^+ \leftarrow X^2\Pi_{3/2}) = P_1(1)(\text{OH}, A^2\Sigma^+ \leftarrow X^2\Pi_{3/2}) + ZPE(\text{OH}, X^2\Pi_{3/2}) - ZPE(\text{OH}, A^2\Sigma^+)$  (where ZPE includes the anharmonic vibrational zero-point energy,



the  $Y_{00}$  term, and the rotational term of the lowest allowed level) be the term energy of the bottom of the  $A^2\Sigma^+$  well relative to the bottom of the  $X^2\Pi_{3/2}$  well. If the electronic isotope shifts of  $X^2\Pi_{3/2}$  and  $A^2\Sigma^+$  were the same, OH and OD should produce exactly the same value for  $T_e$ . However, based on data and constants listed in Huber and Herzberg,<sup>40</sup>  $T_e(\text{OH}, A^2\Sigma^+ \leftarrow X^2\Pi_{3/2}) = 32685.64 \text{ cm}^{-1}$  and  $T_e(\text{OD}, A^2\Sigma^+ \leftarrow X^2\Pi_{3/2}) = 32681.24 \text{ cm}^{-1}$ , differing by  $4.4 \text{ cm}^{-1}$ . Hence, in going from OH to OD, one of the two states shifts  $4.4 \text{ cm}^{-1}$  more than the other. The individual shifts of  $X^2\Pi_{3/2}$  and  $A^2\Sigma^+$  could be substantially larger, as long as their difference is  $4.4 \text{ cm}^{-1}$ . Hence, a shift as large as  $20 \text{ cm}^{-1}$  in  $X^2\Pi_{3/2}$  is perhaps not entirely out of the question.

(79) The reported<sup>15,69</sup>  $\Delta G(0.5)$  and  $\Delta G(1.5)$  values for OD are just sufficient to obtain  $\omega_e$  and  $\omega_e x_e$ . Using the isotopic relations  $\omega_e(\text{OH}) = f \times \omega_e(\text{OD})$  and  $\omega_e x_e(\text{OH}) = f^2 \times \omega_e x_e(\text{OD})$ , where  $f = 1.373465$  is the square root of the ratio of reduced masses of OD and OH, the constants obtained from OD quite closely reproduce  $\Delta G(0.5)$  of OH. Slightly more refined values are obtained by a least-squares fit of all three  $\Delta G(v + 1/2)$  values, leading to  $\omega_e(\text{OH}) = 1015.4 \text{ cm}^{-1}$  and  $\omega_e x_e(\text{OH}) = 179.2 \text{ cm}^{-1}$ .

(80) If more information were available on the B state, one could, at least in principle, use a more sophisticated form of the potential than the Morse curve. However, the second term in eq 7 is also just an approximate estimate of the rotational energy. When using effective potential curves, the actual rotational levels should correspond to the sum of the energy of the minimum of the potential curve and the vibrational energy.<sup>36</sup> This is generally not quite true, because a good representation of the rotational energy typically includes higher terms in  $(v + 1/2)$  and  $J(J + 1)$ .

(81) Werner, H.-J.; Knowles, P. J. *J. Chem. Phys.* **1985**, *82*, 5053. Knowles, P. J.; Werner, H.-J. *Chem. Phys. Lett.* **1985**, *115*, 259. Werner, H.-J.; Knowles, P. J. *J. Chem. Phys.* **1988**, *89*, 5803. Knowles, P. J.; Werner, H.-J. *J. Chem. Phys. Lett.* **1988**, *145*, 514.

(82) Gray, S. 2000, private communication.

(83) The calculated values for the  $A^2\Sigma^+$  state  $D_e = 20120.8 \text{ cm}^{-1}$ ; for OH: ZPE =  $1574.2 \text{ cm}^{-1}$ ,  $D_0 = 18546.6 \text{ cm}^{-1}$ ,  $\Delta G(0.5) = 3001.4 \text{ cm}^{-1}$ ,  $\Delta G(1.5) = 2809.5 \text{ cm}^{-1}$ ,  $\Delta G(2.5) = 2614.6 \text{ cm}^{-1}$ ,  $\Delta G(3.5) = 2415.9 \text{ cm}^{-1}$ ,  $\Delta G(4.5) = 2193.3 \text{ cm}^{-1}$ ,  $\Delta G(5.5) = 1928.0 \text{ cm}^{-1}$ ,  $\Delta G(6.5) = 1592.5 \text{ cm}^{-1}$ ,  $\Delta G(7.5) = 1160.8 \text{ cm}^{-1}$ ,  $\Delta G(8.5) = 633.6 \text{ cm}^{-1}$ , and  $\Delta G(9.5) = 181.6 \text{ cm}^{-1}$ ; for OD: ZPE =  $1150.2 \text{ cm}^{-1}$ ,  $\Delta G(0.5) = 2222.9 \text{ cm}^{-1}$ ,  $\Delta G(1.5) = 2122.3 \text{ cm}^{-1}$ ,  $\Delta G(2.5) = 2018.8 \text{ cm}^{-1}$ ,  $\Delta G(3.5) = 1916.7 \text{ cm}^{-1}$ ,  $\Delta G(4.5) = 1813.0 \text{ cm}^{-1}$ ,  $\Delta G(5.5) = 1702.6 \text{ cm}^{-1}$ ,  $\Delta G(6.5) = 1581.3 \text{ cm}^{-1}$ ,  $\Delta G(7.5) = 1442.1 \text{ cm}^{-1}$ ,  $\Delta G(8.5) = 1277.4 \text{ cm}^{-1}$ ,  $\Delta G(9.5) = 1080.2 \text{ cm}^{-1}$ ,  $\Delta G(10.5) = 842.9 \text{ cm}^{-1}$ ,  $\Delta G(11.5) = 565.5 \text{ cm}^{-1}$ ,  $\Delta G(12.5) = 282.0 \text{ cm}^{-1}$ , and  $\Delta G(13.5) = 90.0 \text{ cm}^{-1}$ .

(84) Interestingly, the information contained in the experimental  $B_v$  values given by Carlone and Dalby also suggests that the Birge–Spencer extrapolation of the experimental  $\Delta G(v + 1/2)$  values underestimates the  $(v + 1/2)_{\text{intercept}}$  by at least 0.5. As one climbs up the vibrational ladder, the rotational constants become smaller on account of the increasing internuclear distance. At the dissociation limit, the internuclear distance becomes infinite and the rotational constant goes to zero. The experimental rotational constants can also be represented by a Dunham polynomial expansion in  $v + 1/2$ , which can then be extrapolated to zero producing  $v_{\text{max}}$ . If the Dunham expansion were completely valid, both  $G(v)$  and  $B(v)$  would yield the same value for  $v_{\text{max}}$ . However, the average values for  $v_{\text{max}}$  from fits of rotational constants for the A state using 4th, 5th, and 6th order polynomial are 10.559 for OH and 14.391 for OD, slightly more than 0.5 larger than those obtained from the Birge–Spencer fit of the vibrational gaps. Unfortunately, there is no transparent way to convert these  $v_{\text{max}}$  values into useful estimate of the dissociation energy, because they exceed the  $v_{\text{max}}$  values supported by the  $G(v)$  expressions. In fact, because the fit of rotational constants is subject to the same criticism as the Birge–Spencer extrapolation, the resulting  $v_{\text{max}}$  is probably a lower limit to the proper value.

(85) Le Roy, R. J.; Bernstein, R. B. *Chem. Phys. Lett.* **1970**, *5*, 42. Le Roy, R. J.; Bernstein, R. B. *J. Chem. Phys.* **1970**, *52*, 3869. Le Roy, R. J.; Bernstein, R. B. *J. Mol. Spectrosc.* **1971**, *37*, 109. Le Roy, R. J. In *Molecular Spectroscopy*; Barrow, R. F., Long, D. A., Millen, D. J., Eds.; Chemical Society: London, 1973; Vol. 1, p 113. Le Roy, R. J. *Can. J. Phys.* **1972**, *50*, 953. Le Roy, R. J. *J. Chem. Phys.* **1980**, *73*, 6003.

(86) Stwalley, W. C. *Chem. Phys. Lett.* **1970**, *6*, 241. Stwalley, W. C. *J. Chem. Phys.* **1973**, *58*, 3867. Stwalley, W. C.; Uang, Y. H.; Pichler, G. *Phys. Rev. Lett.* **1978**, *41*, 1164.

(87) Le Roy, R. J.; Lam, W.-H. *Chem. Phys. Lett.* **1980**, *71*, 544. Tromp, J. W.; Le Roy, R. J. *Can. J. Phys.* **1982**, *60*, 26.

(88) Hashemi-Attar, A.-R.; Beckel, C. L.; Keepin, W. N.; Sonnleitner, S. A. *J. Chem. Phys.* **1979**, *70*, 3881. A.-R. Hashemi-Attar, A.-R.; Beckel, C. L. *J. Chem. Phys.* **1979**, *71*, 4596. Beckel, C. L.; Kwong, R. B. *J. Chem. Phys.* **1980**, *73*, 4698. Beckel, C. L.; Kwong, R. B.; Hashemi-Attar, A.-R.; Le Roy, R. J. *J. Chem. Phys.* **1984**, *81*, 66.

(89) Le Roy, R. J.; Barwell, M. G. *Can. J. Phys.* **1975**, *53*, 1983. Tromp, J. W.; Le Roy, R. J. *J. Mol. Spectrosc.* **1985**, *109*, 352. Jordan, K. J.; Lipsch, R. H.; McDonald, N. A.; Le Roy, R. J. *J. Phys. Chem.* **1992**, *96*, 4778.

(90) Field, R. W. 2000, private communication.

(91) The numerical results quoted in this section refer to RKR points that were calculated by using a 5th order Dunham expansion for  $G(v)$  and

a 4th order Dunham expansion for  $B(v)$ ; the polynomials were obtained by fitting vibrational energies and rotational constants for  $v = 0-9$  in OH and  $v = 0-13$  in OD that are given in ref 15.

(92) We have used the following expressions:  $G(v) = D_e - X_0(n)(v_{\text{max}} - v)^{2n/(n-2)}[L/M]^s$ ;  $X_0(n) = (\mu^n C_n 2)^{1/(2-n)} [h(n-2)(8\pi)^{1/2} \Gamma(1+1/n) \Gamma(1/2+1/n)]^{2n/(n-2)} L = 1 + p_1(v_{\text{max}} - v) + p_2(v_{\text{max}} - v)^2 + \dots + p_L(v_{\text{max}} - v)^L$ ;  $M = 1 + q_1(v_{\text{max}} - v) + q_2(v_{\text{max}} - v)^2 + \dots + q_L(v_{\text{max}} - v)^L$  where  $D_e$  is the dissociation limit,  $n$  is the leading inverse power of  $r$ ,  $C_n$  is the leading long-range coefficient,  $v_{\text{max}}$  is the effective noninteger vibrational index at the dissociation limit,  $\mu$  is the reduced mass, and  $\Gamma(x)$  is the standard gamma function.  $[L/M]$  is a Padé approximant.  $s = 1$  produces the “outer” Padé expansion and  $s = 2n/(n-2)$  produces the “inner” Padé expansion. See refs 85–89 for more details.

(93) Werner, H. J.; Knowles, P. J.; Almlof, J.; Amos, R. D.; Berning, A.; Cooper, D. L.; Deegan, M. J. O.; Dobbyn, A. J.; Eckart, F.; Elbert, S. T.; Hampel, C.; Lindh, R.; Lloyd, A. W.; Meyer, W.; Nekliss, A.; Peterson, K. A.; Pitzer, R. M.; Stone, A. J.; Taylor, P. R.; Mura, M. E.; Pulay, P.; Schütz, M.; Stoll, H.; Thorsteinsson, T. *MOLPRO-2000*, Universität Stuttgart, Stuttgart, Germany, and University of Sussex, Falmer, Brighton, England, 1997.

(94) Frisch, M. J.; Trucks, G. W.; Schlegel, H. B.; Scuseria, G. E.; Robb, M. A.; Cheeseman, J. R.; Zakrzewski, V. G.; Montgomery, J. A., Jr.; Stratmann, R. E.; Burant, J. C.; Dapprich, S.; Millam, J. M.; Daniels, A. D.; Kudin, K. N.; Strain, M. C.; Farkas, O.; Tomasi, J.; Barone, V.; Cossi, M.; Cammi, R.; Mennucci, B.; Pomelli, C.; Adamo, C.; Clifford, S.; Ochterski, J.; Petersson, G. A.; Ayala, P. Y.; Cui, Q.; Morokuma, K.; Malick, D. K.; Rabuck, A. D.; Raghavachari, K.; Foresman, J. B.; Cioslowski, J.; Ortiz, J. V.; Stefanov, B. B.; Liu, G.; Liashenko, A.; Piskorz, P.; Komaromi, I.; Gomperts, R.; Martin, R. L.; Fox, D. J.; Keith, T.; Al-Laham, M. A.; Peng, C. Y.; Nanayakkara, A.; Gonzalez, C.; Challacombe, M.; Gill, P. M. W.; Johnson, B. G.; Chen, W.; Wong, M. W.; Andres, J. L.; Head-Gordon, M.; Replogle, E. S.; Pople, J. A. *Gaussian 98*, revision A.7; Gaussian, Inc.: Pittsburgh, PA, 1998.

(95) ACES II is a program product of the Quantum Theory Project, University of Florida, 1998. Authors: Gauss, J.; Watts, J. D.; Nooijen, M.; Oliphant, N.; Perera, S. A.; Szalay, P. G.; Lauderdale, W. J.; Gwaltney, S. R.; Beck, S.; Balkova, A.; Bernholdt, D. E.; Baeck, K.-K.; Rozyczko, P.; Sekino, H.; Hober, C.; Bartlett, R. J. Integral packages include VMOL (Almlof, J.; Taylor, P. R.); VPROPS (Taylor, P. R.); ABACUS (Helgaker, T.; Jensen, H. J. A.; Jørgensen, P.; Olsen, J. and Taylor, P. R.) computer programs.

(96) Valeev E.; Allen W. D. 1999 private communication.

(97) Hampel, C.; Peterson, K. A.; Werner, H. J. *Chem. Phys. Lett.* **1990**, *190*, 1. Deegan, M. J. O.; Knowles, P. J. *J. Chem. Phys. Lett.* **1994**, *227*, 321. Knowles, P. J.; Hampel, C.; Werner, H. J. *J. Chem. Phys.* **1988**, *99*, 5219.

(98) Rittby, M.; Bartlett, R. J. *J. Phys. Chem.* **1988**, *92*, 3033; R/UCCSD(T) is requested in MOLPRO by the keyword “UCCSD(T)” when combined with an ROHF wave function.

(99) Feller, D. *J. Chem. Phys.* **1999**, *111*, 4373.

(100) Feller, D.; Sordo, J. A. *J. Chem. Phys.* **2000**, *112*, 5604.

(101) Feller, D.; Sordo, J. A. *J. Chem. Phys.* **2000**, *113*, 485.

(102) Knowles, P. J. *Chem. Phys. Lett.* **1989**, *155*, 513.

(103) Feller, D.; Dixon, D. A. *J. Phys. Chem. A* **2000**, *104*, 3048.

(104) Noga, J.; Bartlett, R. J. *J. Chem. Phys.* **1987**, *86*, 7041. Scuseria, G. E.; Schaefer, H. F., III. *Chem. Phys. Lett.* **1988**, *152*, 382. Watts, J. D.; Bartlett, R. J. *J. Chem. Phys.* **1990**, *93*, 6104. Watts, J. D.; Bartlett, R. J. *Int. J. Quantum Chem. Symp.* **1993**, *27*, 51.

(105) Klopper, W.; Bak, K. L.; Jørgensen, P. J.; Olsen, J.; Helgaker, T. *J. Phys. B* **1999**, *32*, R103.

(106) Schwartz, C. In *Methods in Computational Physics*; Alder, B. J., Fernbach, S., Rotenberg, M., Eds.; Academic Press: New York, 1963; Vol. 2; p 262. Martin, J. M. L. *Chem. Phys. Lett.* **1996**, *259*, 669.

(107) Helgaker, T.; Klopper, W.; Koch, H.; Nagel, J. *J. Chem. Phys.* **1997**, *106*, 9639. Halkier, A.; Helgaker, T.; Jørgensen, P.; Klopper, W.; Koch, H.; Olsen, J.; Wilson, A. K. *Chem. Phys. Lett.* **1998**, *286*, 243.

(108) Peterson, K. A.; Woon, D. E.; Dunning, T. H., Jr. *J. Chem. Phys.* **1994**, *100*, 7410.

(109) This choice is supported by the results of extrapolations using eq 9d, which is expected to underestimate the CBS total energies. Using the 5- $\zeta$  through 7- $\zeta$  basis sets, this “mixed” formula yields  $D_e(\text{H-OH})$  and  $D_e(\text{OH})$  values of 125.59 and 106.97 kcal/mol, respectively, which differ from our best estimates by  $-0.09$  and  $-0.12$  kcal/mol, respectively.

(110) Herzberg, G. *Molecular Spectra and Molecular Structure II. Infrared and Raman Spectra of Polyatomic Molecules*; Van Nostrand: New York, 1945.

(111) The value can be obtained by using constants from ref 39 (including the spin-orbit splitting constant  $A_0 = -139.21 \text{ cm}^{-1}$ ) and the Van Vleck expression given in ref 35, leading to  $F_1(3/2) = -38.19 \text{ cm}^{-1}$  and  $F_2(1/2) = 88.15 \text{ cm}^{-1}$ , which correctly reproduces the experimental splitting  $X^2\Pi_{1/2} v = 0, J = 1/2 \leftarrow X^2\Pi_{3/2} v = 0, J = 3/2$  of  $126.23 \text{ cm}^{-1}$ .

(112) Davidson, E. R.; Ishikawa, Y.; Malli, G. L. *Chem. Phys. Lett.* **1981**, *84*, 226.

(113) Schwenne, D. W., *J. Phys. Chem. A* **2001**, *105*, 2352.



- (114) Handy, N. C.; Lee, A. M. *Chem. Phys. Lett.* **1996**, 252, 425.
- (115) In the present work, the difference between using nuclear masses instead of atomic masses in the BODC is negligible.
- (116) Noga, J.; Valiron, P.; Klopper, W. *J. Chem. Phys.* **2001**, 115, 2022.
- (117) Martin, J. M. L. *Spectrosc. Acta Part A* **2001**, 57, 875.
- (118) Smith, J. R.; Kim, J. B.; Lineberger, W. C. *Phys. Rev. A* **1997**, 55, 2036. See also: Schulz, P. A.; Mead, R. D.; Jones, P. L.; Lineberger, W. C. *J. Chem. Phys.* **1982**, 77, 1153.
- (119) Mallard, W. G.; Linstrom, P. J., Eds.; *NIST Chemistry WebBook*, NIST Standard Reference Database Number 69, February 2000; National Institute of Standards and Technology: Gaithersburg MD, 2000 (<http://webbook.nist.gov>).
- (120) Blondel, C. *Phys. Scr. T* **1995**, T58, 31. See also: Neumark, D. M.; Lykke, K. R.; Andersen, T.; Lineberger, W. C. *Phys. Rev. A* **1985**, 32, 1890.
- (121) Hunter, E. P.; Lias, S. G. *J. Phys. Chem. Ref. Data* **1998**, 27, 413.
- (122) These are derived, not measured, quantities. However, it is not unequivocally clear which values for the enthalpy of formation of OH, as well as IE(OH) and IE(H<sub>2</sub>O), were used to obtain the listed values for PA(O) and PA(OH) listed in ref 121. Reference is given there to Lias, S. G.; Bartmess, J. E.; Liebman, J. F.; Holmes, J. L.; Levin, R. D.; Mallard, W. G. *J. Phys. Chem. Ref. Data* **1988**, 17, Suppl. 1, but from the 298 K enthalpies listed there we obtain PA(OH) = 142.0 kcal/mol and PA(O) = 116.2 kcal/mol. This source uses the JANAF 298 K enthalpy of OH of 9.3 kcal/mol (which is not only based on an unexplained 0 K value but also uses a wrong 0–298 K conversion, see refs 17 and 18). It should be also noted that, if our values and those in ref 121 differed only in the choice of  $\Delta H_f^\circ(\text{OH})$ , then the sum PA(O) + PA(OH) should be the same in both cases. After some trial and error, we have concluded that the values used must have been 9.3 kcal/mol for the 298 K enthalpy of OH, 13.01 eV as the IE(OH), and 12.62 eV as IE(H<sub>2</sub>O). The IEs would appear to correspond in both cases to prevailing PES values.
- (123) Tonkyn, R. G.; Wiedmann, R.; Grant, E. R.; White, M. G. *J. Chem. Phys.* **1991**, 95, 7033. This value is slightly lower than previous values, see, e.g.: Page, R. H.; Larkin, R. J.; Yhen, Y. R.; Lee, Y. T. *J. Chem. Phys.* **1988**, 88, 2249 and subsequent analysis by Child, M. S.; Jungen, Ch. *J. Chem. Phys.* **1990**, 93, 7756.
- (124) Ruscic, B.; Litorja, M. *Chem. Phys. Lett.* **2000**, 316, 45.
- (125) Bowman, C. T.; Hanson, R. K.; Davidson, D. F.; Gardiner, J. W. C.; Yang, H.; Qin, Z.; Lassianski, V.; Smith, G. P.; Golden, D. M.; Crosley, D.; Frenklach, M.; Moriarty, N. W.; Eiteneer, B.; Wang, H.; Goldenberg, M. in <http://www.gri.org>, 1995.
- (126) Grotheer, H.; Kelm, S.; Driver, H. S. T.; Hutcheon, R. J.; Lockett, R. D.; Robertson, G. N. *Ber. Bunsen-Ges. Phys. Chem.* **1992**, 96, 1360.
- (127) Litorja, M.; Ruscic, B. *J. Chem. Phys.* **1988**, 108, 6748.
- (128) Ruscic, B.; Litorja, M.; Asher, R. L. *J. Phys. Chem. A* **1999**, 103, 8625. see also Erratum, *J. Phys. Chem. A* **2000**, 104, 8600.
- (129) Herbon, J. T.; Hanson, R. K.; Golden, D. M.; Bowman, C. T. submitted to 29th International Symposium on Combustion, to be held in Hokkaido, Japan, July 21–26, 2002.
- (130) Joens, J. A. *J. Phys. Chem. A* **2001**, 105, 11041.
- (131) Luo, X.; Fleming, P. R.; Rizzo, T. R. *J. Chem. Phys.* **1992**, 96, 5659.
- (132) Ruscic, B.; Michael, J. V.; Redfern, P. C.; Curtiss, L. A.; Raghavachari, K. *J. Phys. Chem. A* **1998**, 102, 10889.